This journal is © The Royal Society of Chemistry 2018

Electronic supplementary information

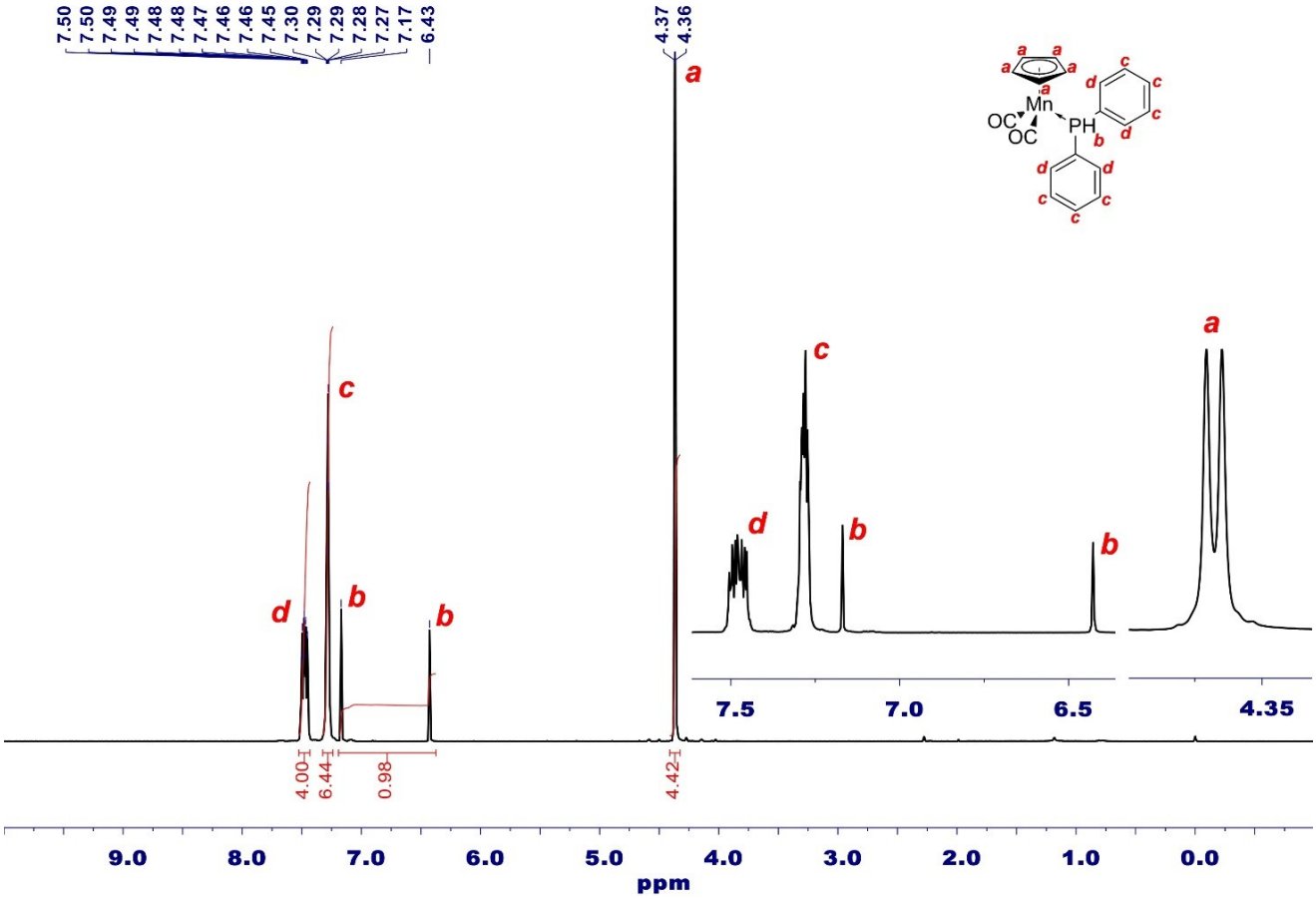

Figure S1. ^{1}H NMR spectrum of $Cp(CO)_2Mn(PPh_2H)$ **3** (400.2 MHz, $CDCl_3$, 25°C)

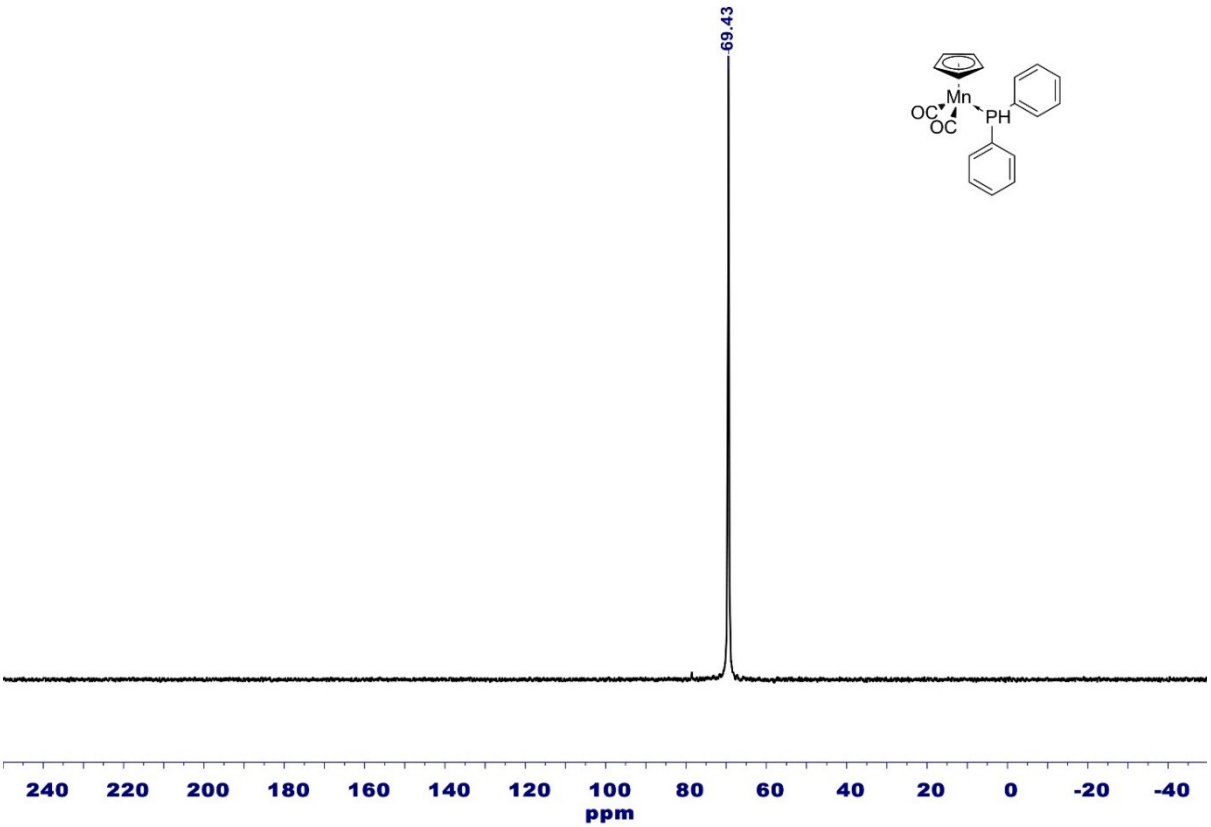

Figure S2. $^{31}P\{^{1}H\}$ NMR spectrum of $Cp(CO)_2Mn(PPh_2H)$ **3** (162.0 MHz, $CDCl_3$, 25°C)

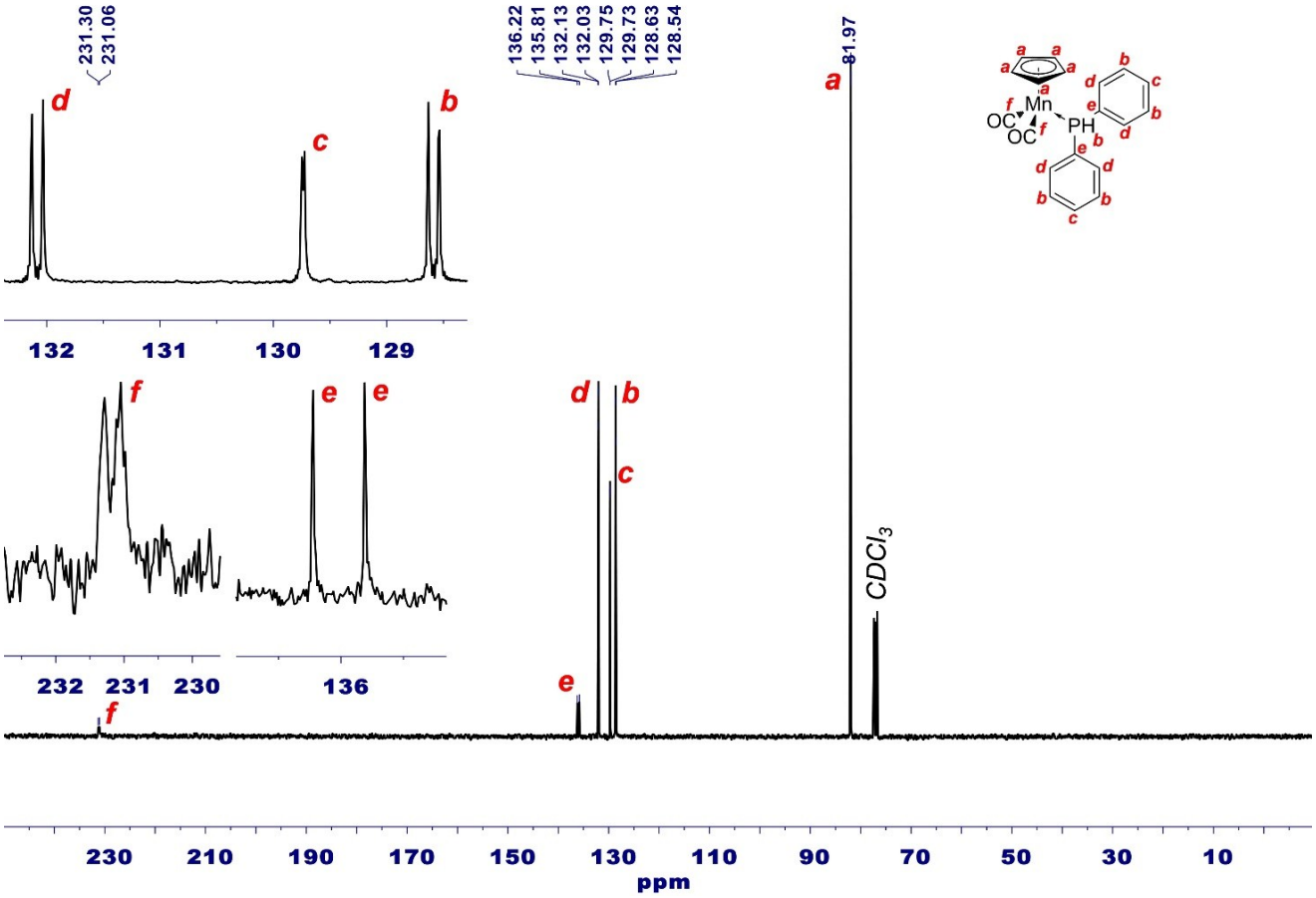

Figure S3. $^{13}C\{^1H\}$ NMR spectrum of $Cp(CO)_2Mn(PPh_2H)$ **3** (100.6 MHz, $CDCl_3$, 25°C)

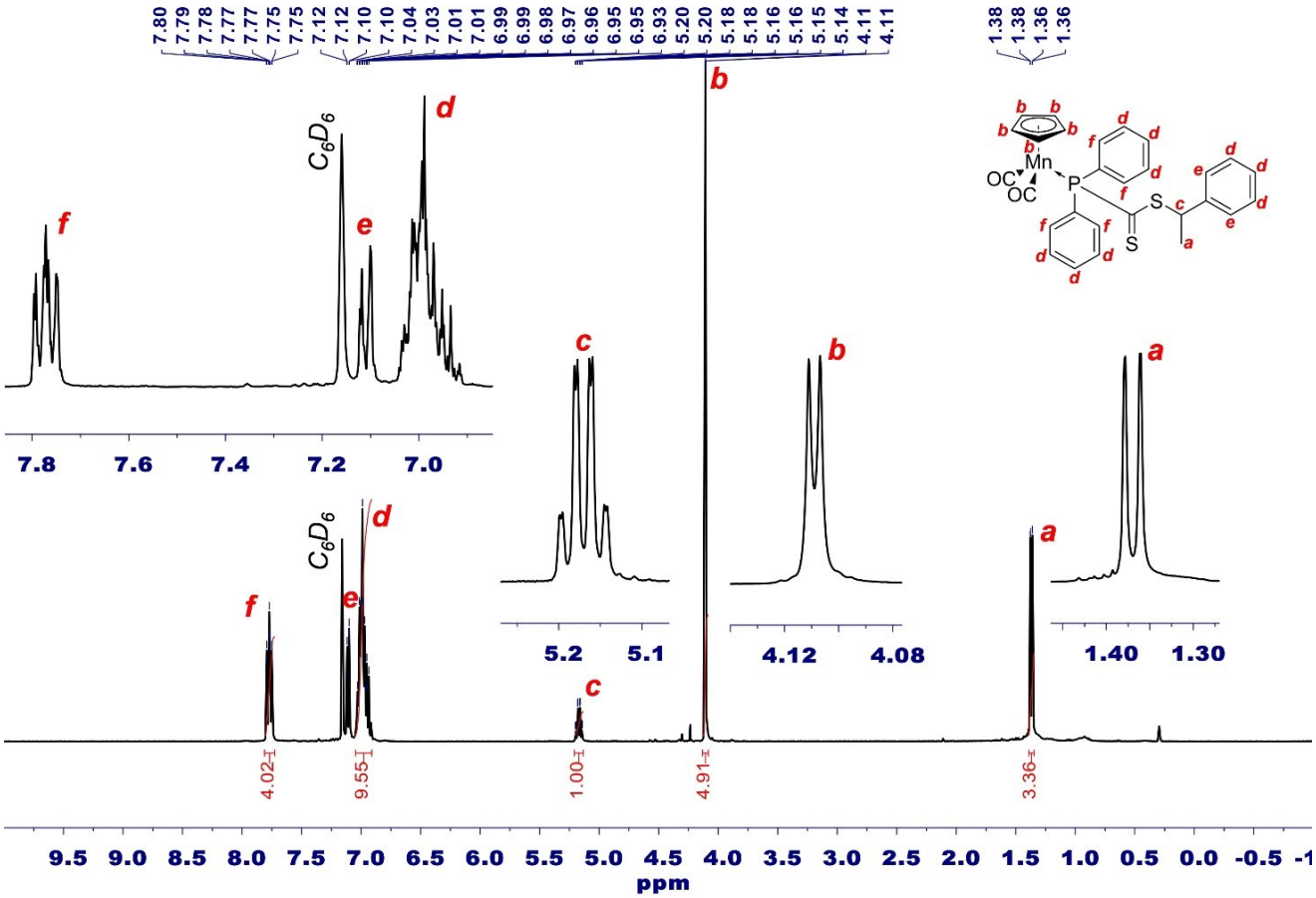

Figure S4. ^1H NMR spectrum of $Cp(CO)_2Mn(PPh_2CS_2CH(Me)Ph)$ **4** (400.2 MHz, $CDCl_3$, 25°C)

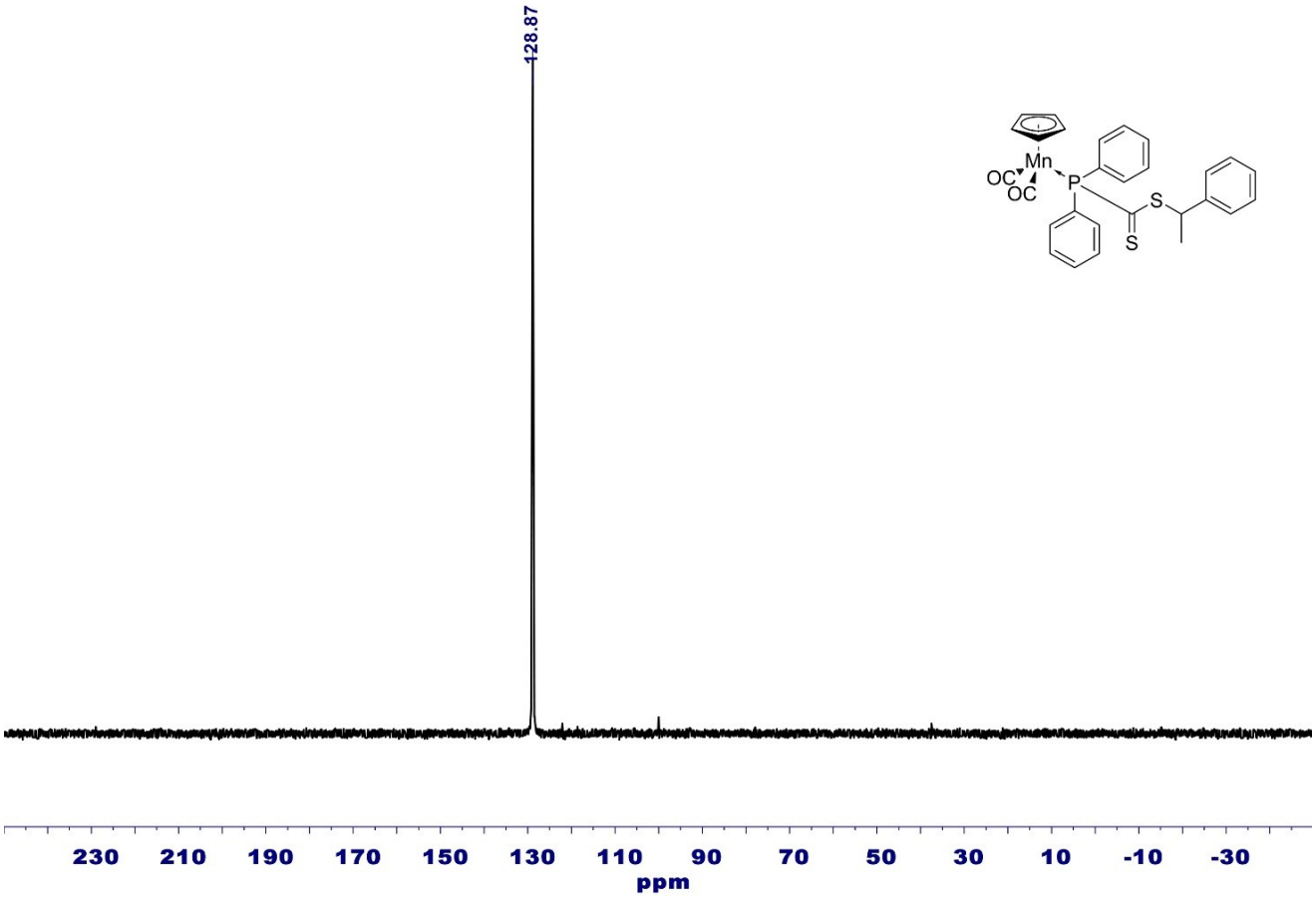

Figure S5. $^{31}P\{^{1}H\}$ NMR spectrum of $Cp(CO)_2Mn(PPh_2CS_2CH(Me)Ph)$ **4** (162.0 MHz, $CDCl_3$, 25°C)

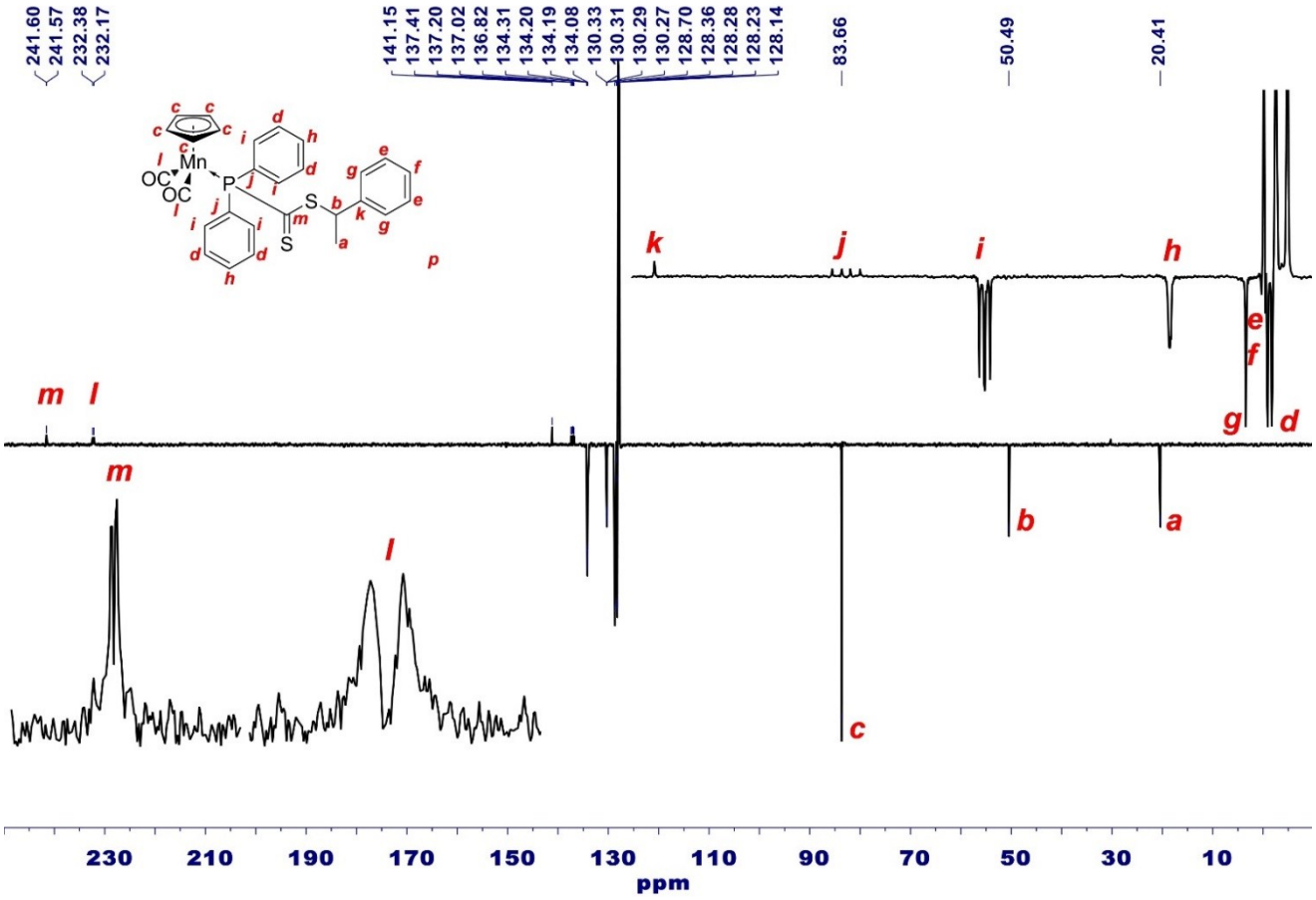

Figure S6. $^{13}C\{^{1}H\}$ NMR spectrum of $Cp(CO)_2Mn(PPh_2CS_2CH(Me)Ph)$ **4** (100.6 MHz, $CDCl_3$, 25°C)

Table S1. Initial reagent concentrations.

Monomer	$[M]_0$, M	$[RAFT]_0$, mM	$[AIBN]_0$, mM	$[M]_0$:$[RAFT]_0$:$[AIBN]_0$
St	6.33	33.9	6.8	187:1:0.2
n-BA	5.09	33.6	6.7	151:1:0.2
DMAAm	6.95	35.4	7.1	196:1:0.2
n-BA [a]	5.09	29.0	5.8	176:1:0.2

[a] Block copolymerization mediated by PSt macro RAFT agent.

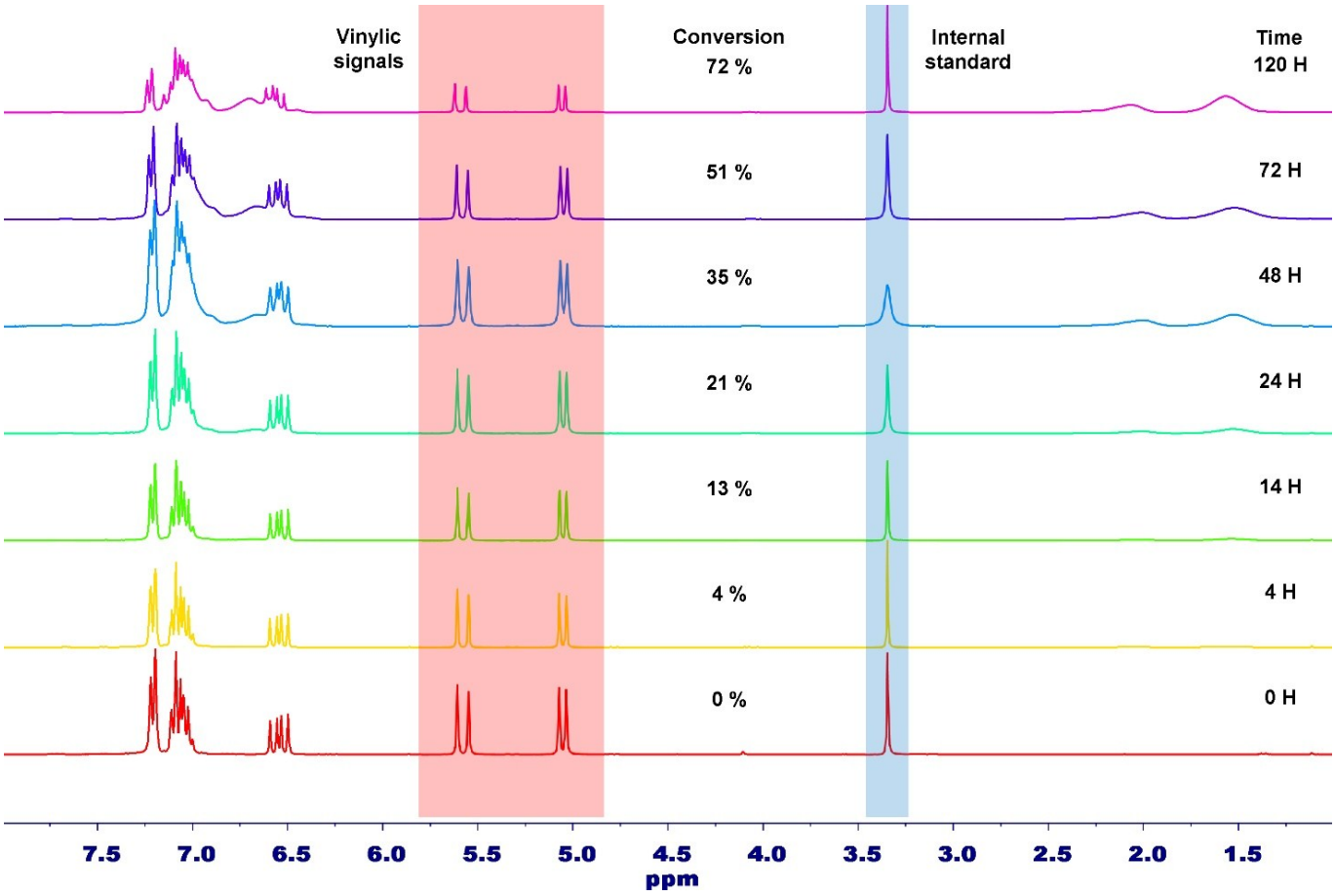

Figure S7. ^{1}H NMR spectra of reaction mixtures obtained during Mn-RAFT mediated St polymerization (300.1 MHz, C_6D_6, 25°C). Each spectrum is fitted to highest intensity.

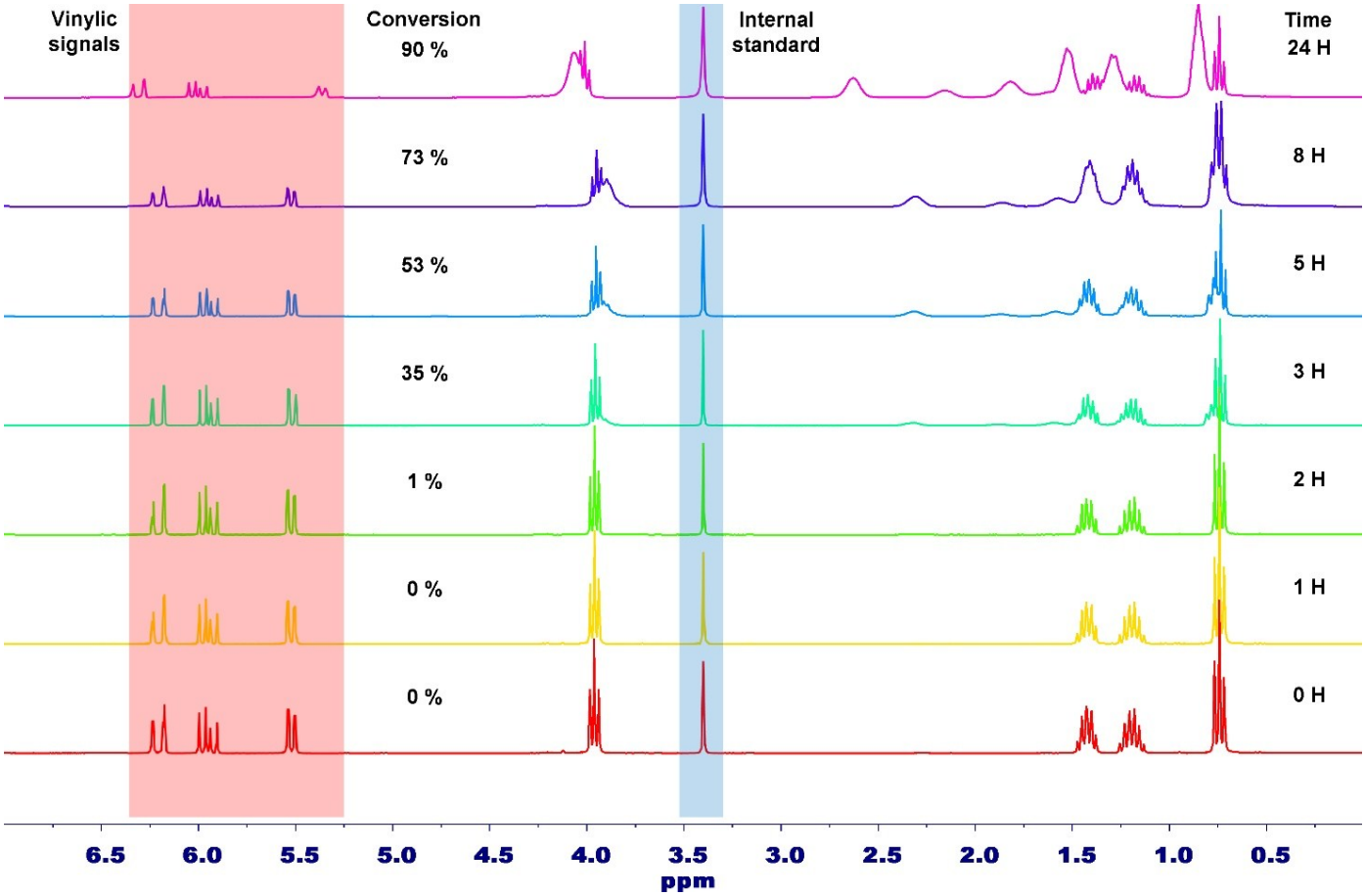

Figure S8. ^{1}H NMR spectra of reaction mixtures obtained during Mn-RAFT mediated *n*-BA polymerization (300.1 MHz, C_6D_6, 25°C). Each spectrum is fitted to highest intensity.

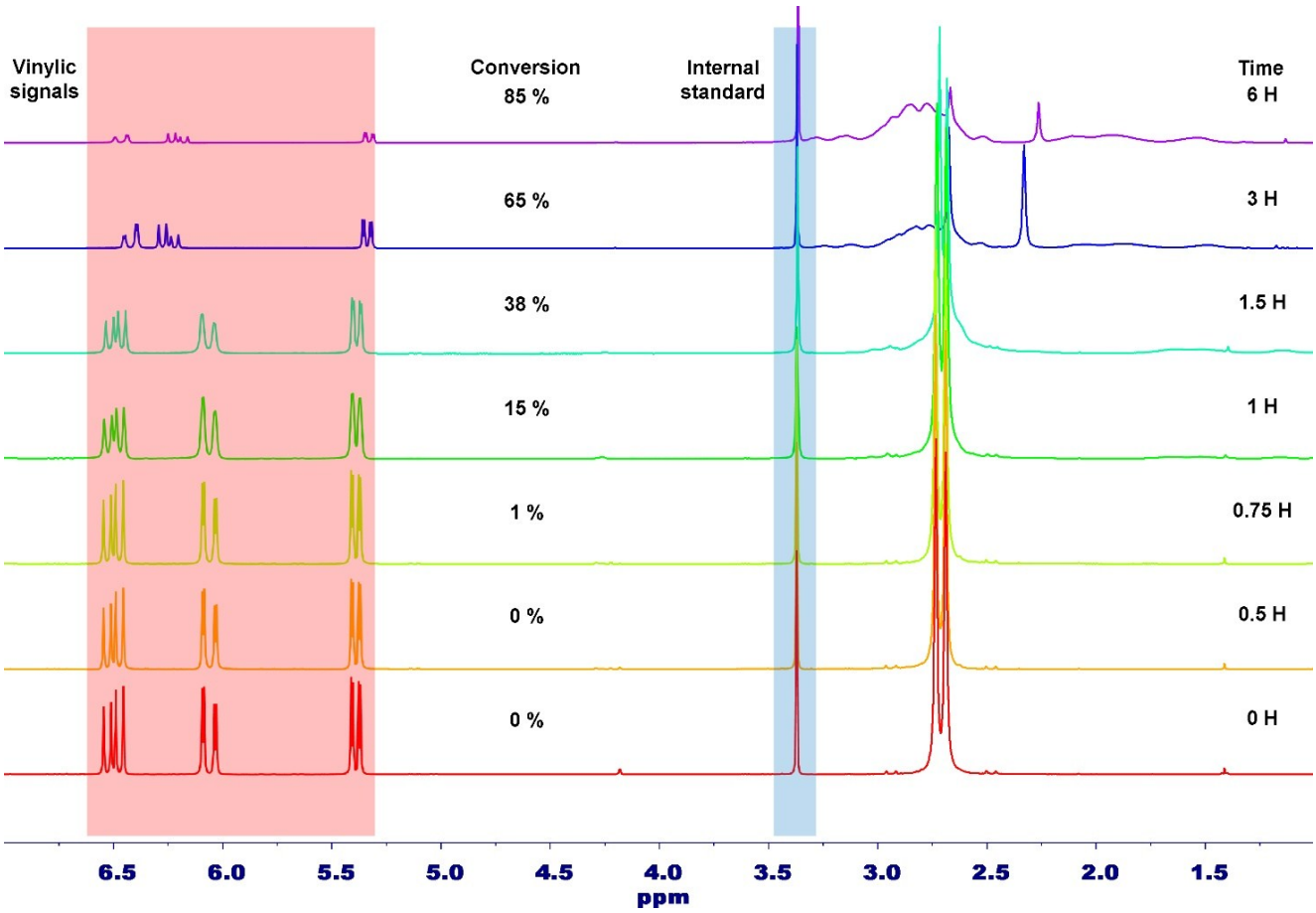

Figure S9. ^{1}H NMR spectra of reaction mixtures obtained during Mn-RAFT mediated DMAAm polymerization (300.1 MHz, C_6D_6, 25°C). Each spectrum is fitted to highest intensity.

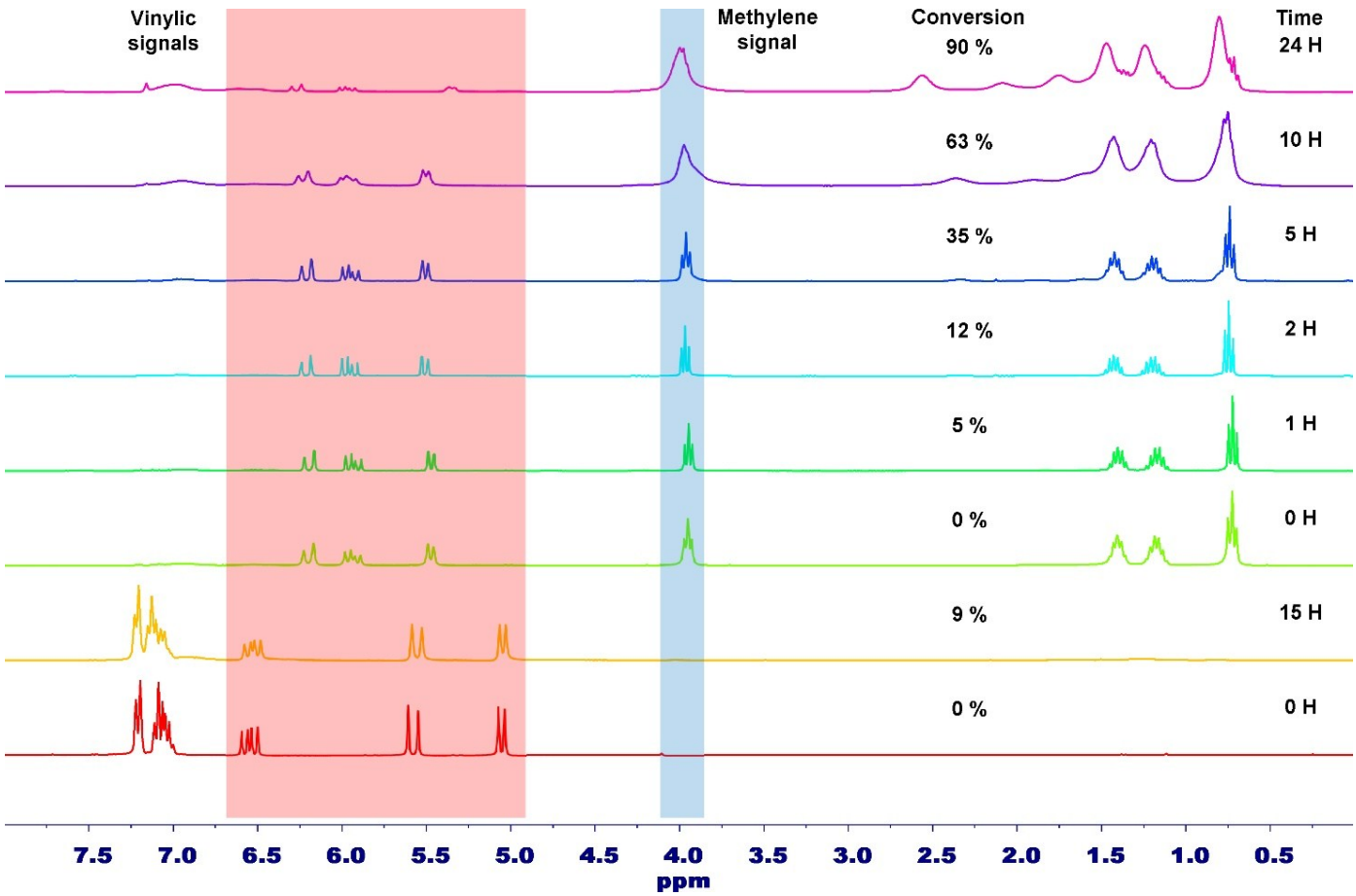

Figure S10. ^{1}H NMR spectra of reaction mixtures obtained during the Mn-RAFT mediated block-copolymerization of St and *n*-BA (300.1 MHz, C_6D_6, 25°C). Each spectrum is fitted to highest intensity.

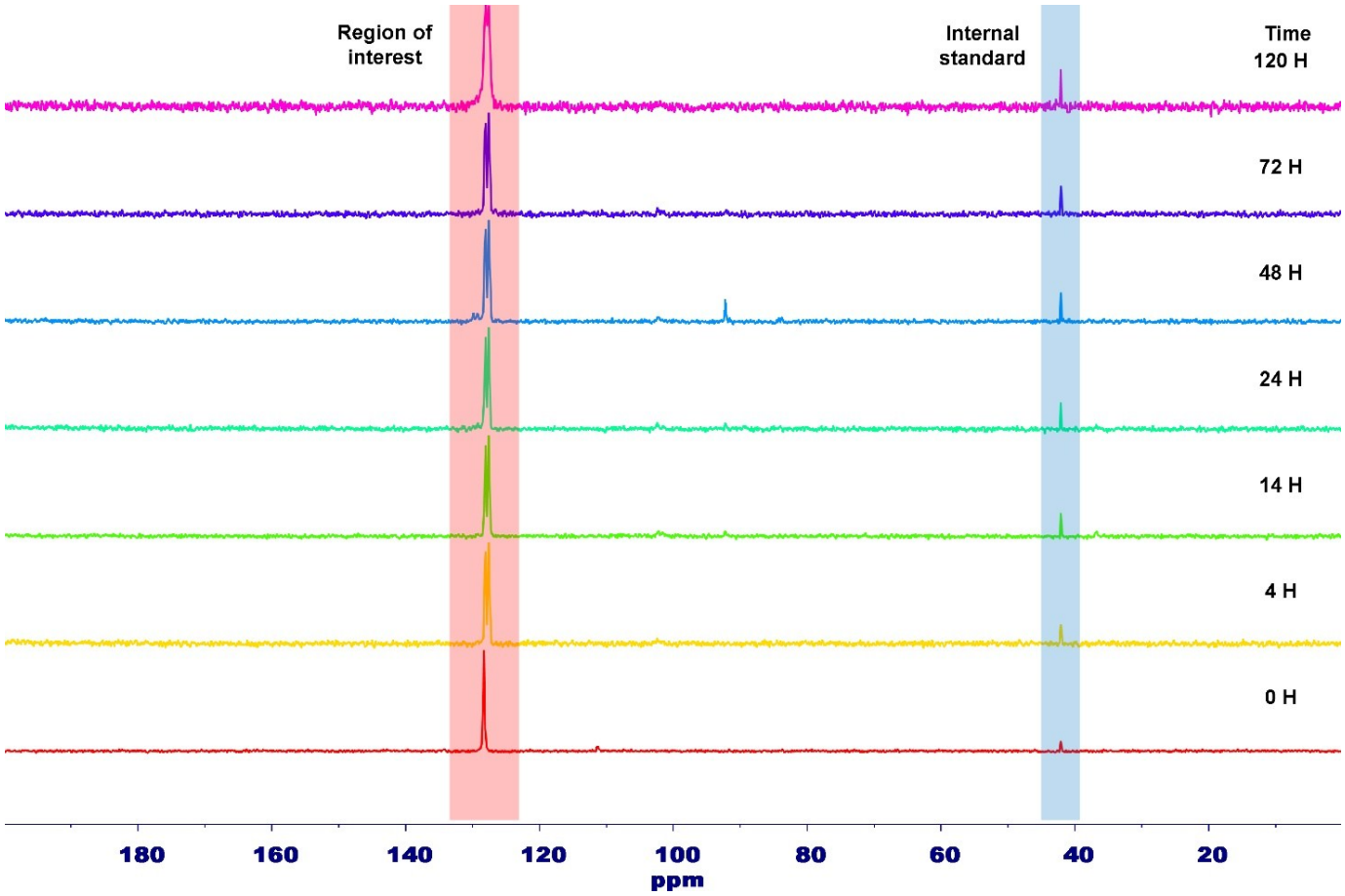

Figure S11. ^{31}P{^{1}H} NMR spectra of reaction mixtures obtained during Mn-RAFT mediated St polymerization (121.5 MHz, C_6D_6, 25°C). Each spectrum is fitted to highest intensity.

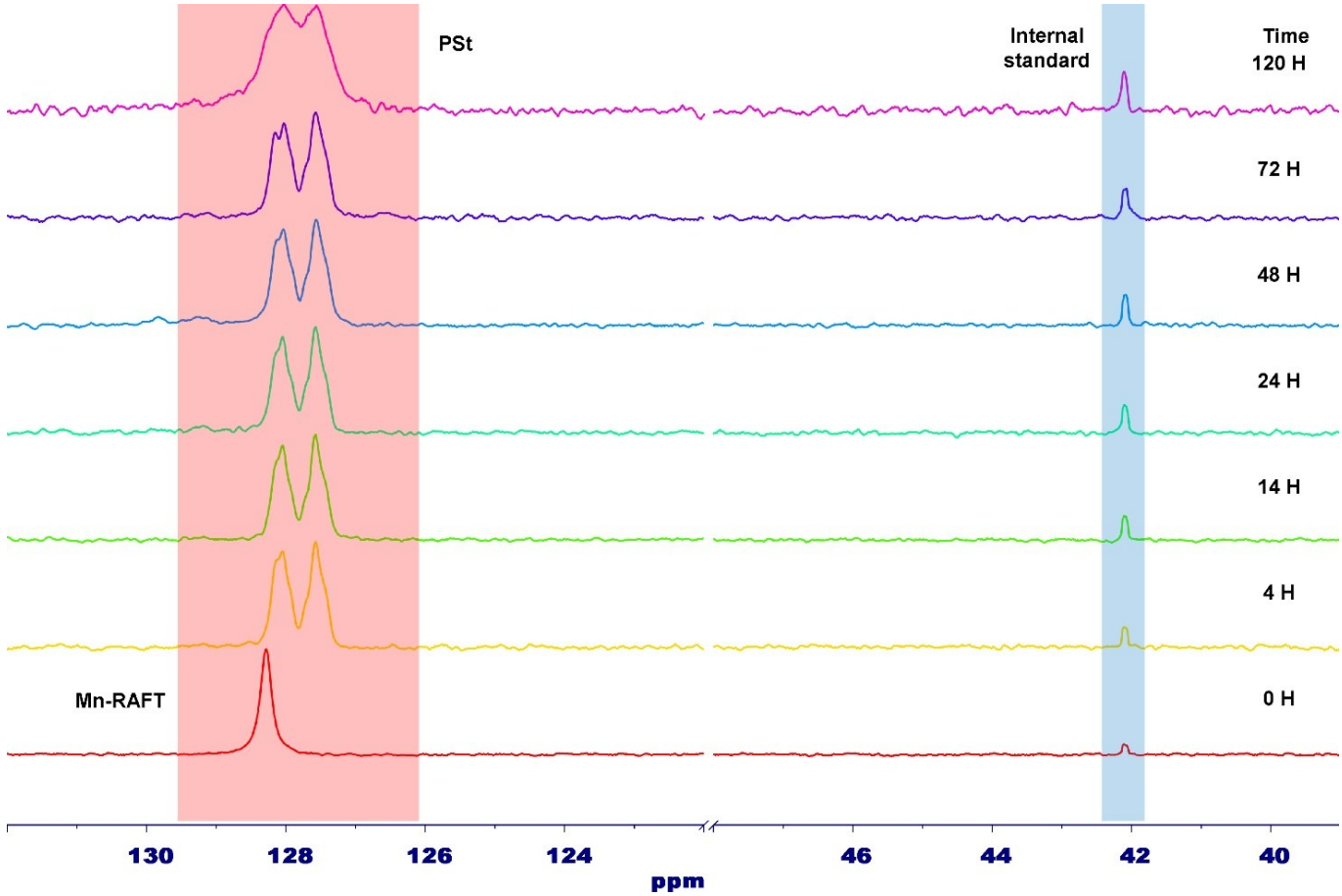

Figure S12. Selected sections of $^{31}P\{^{1}H\}$ NMR spectra of reaction mixtures obtained during Mn-RAFT mediated St polymerization (121.5 MHz, C_6D_6, 25°C). Each spectrum is fitted to highest intensity.

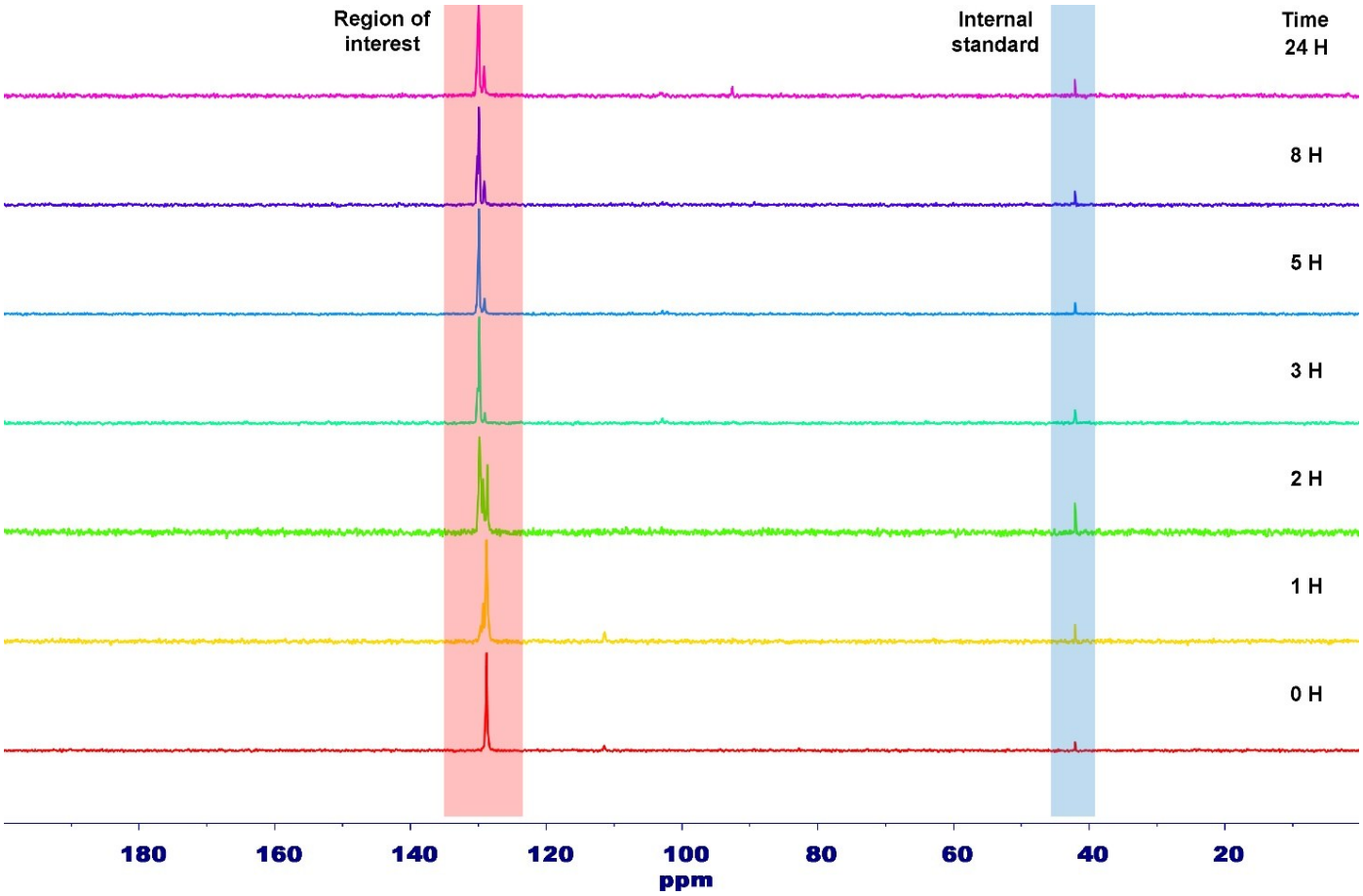

Figure S13. $^{31}P\{^{1}H\}$ NMR spectra of reaction mixtures obtained during Mn-RAFT mediated *n*-BA polymerization (121.5 MHz, C_6D_6, 25°C). Each spectrum is fitted to highest intensity.

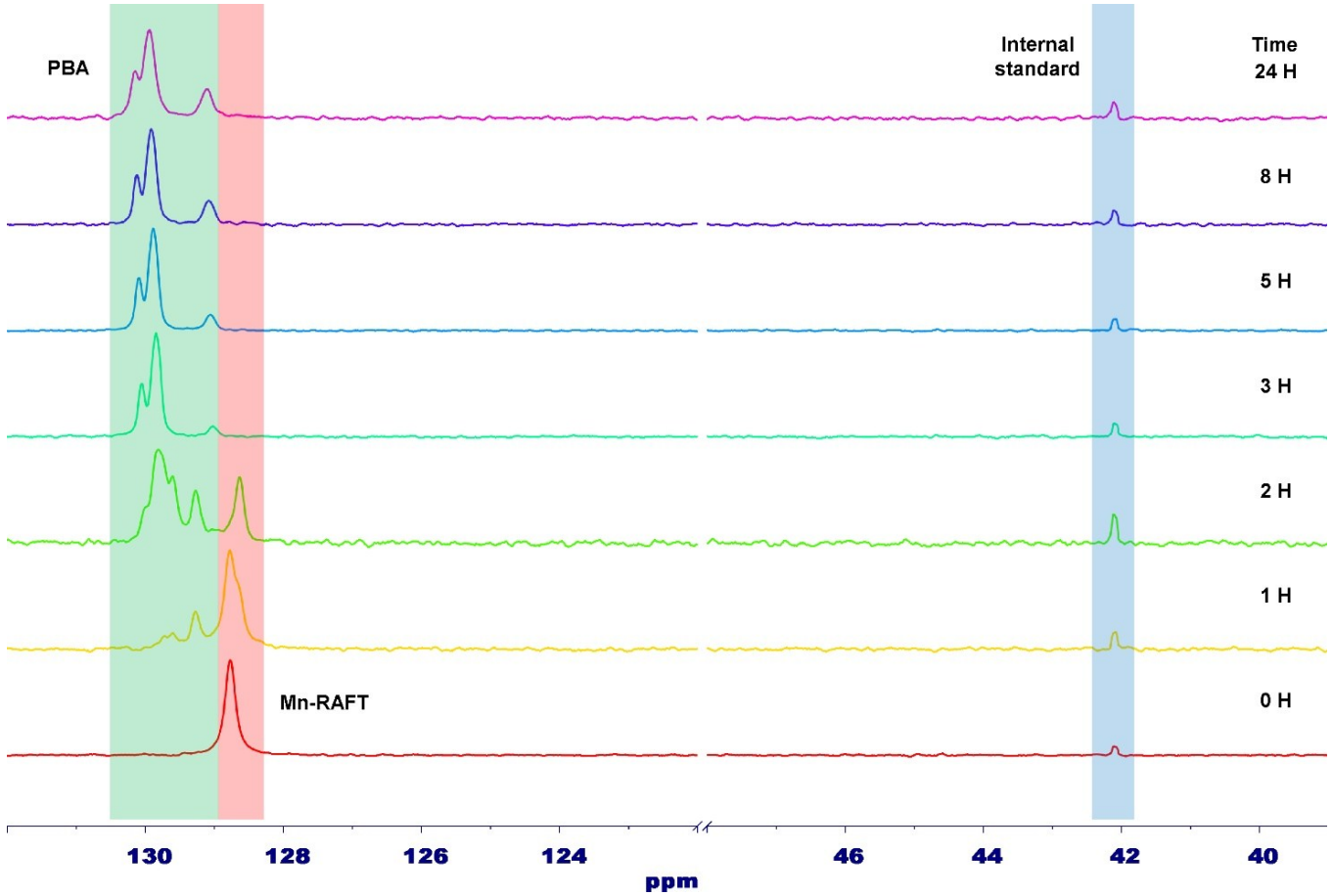

Figure S14. Selected sections of $^{31}P\{^{1}H\}$ NMR spectra of reaction mixtures obtained during Mn-RAFT mediated *n*-BA polymerization (121.5 MHz, C_6D_6, 25°C).-Each spectrum is fitted to highest intensity.

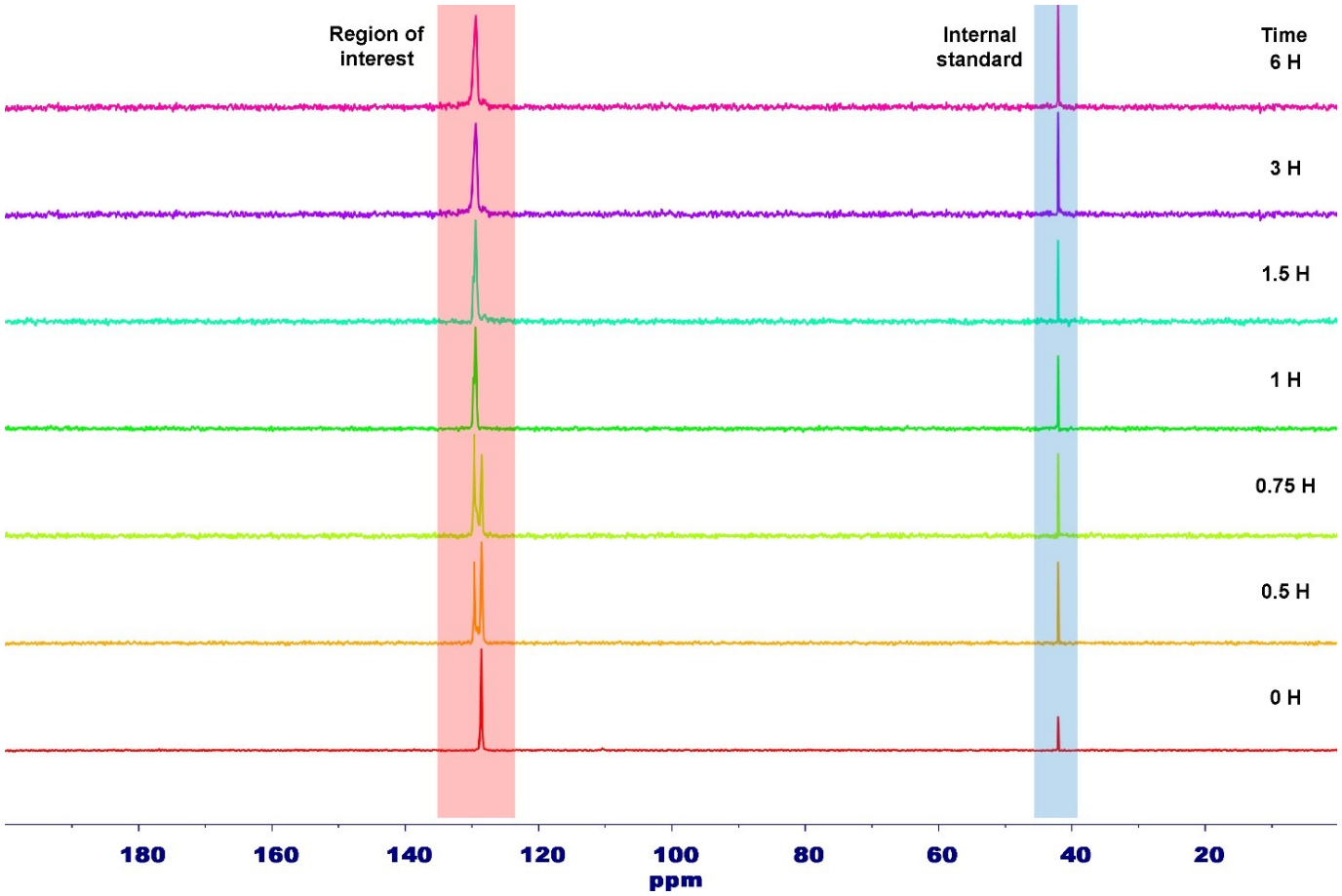

Figure S15. $^{31}P\{^{1}H\}$ NMR spectra of reaction mixtures obtained during Mn-RAFT mediated DMAAm polymerization (121.5 MHz, C_6D_6, 25°C). Each spectrum is fitted to highest intensity.

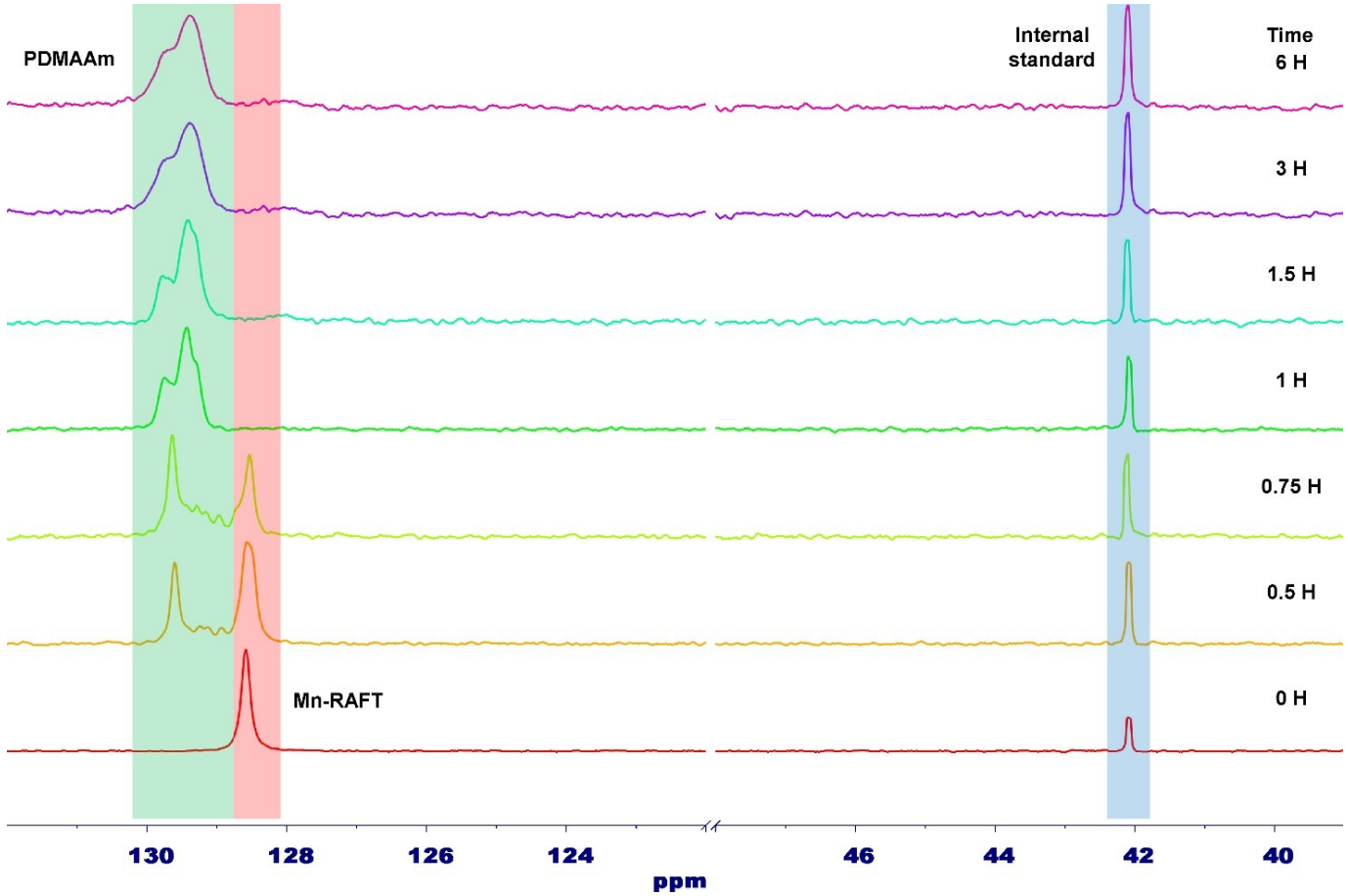

Figure S16. Selected sections of $^{31}P\{^{1}H\}$ NMR spectra of reaction mixtures obtained during Mn-RAFT mediated DMAAm polymerization (121.5 MHz, C_6D_6, 25°C). Each spectrum is fitted to highest intensity.

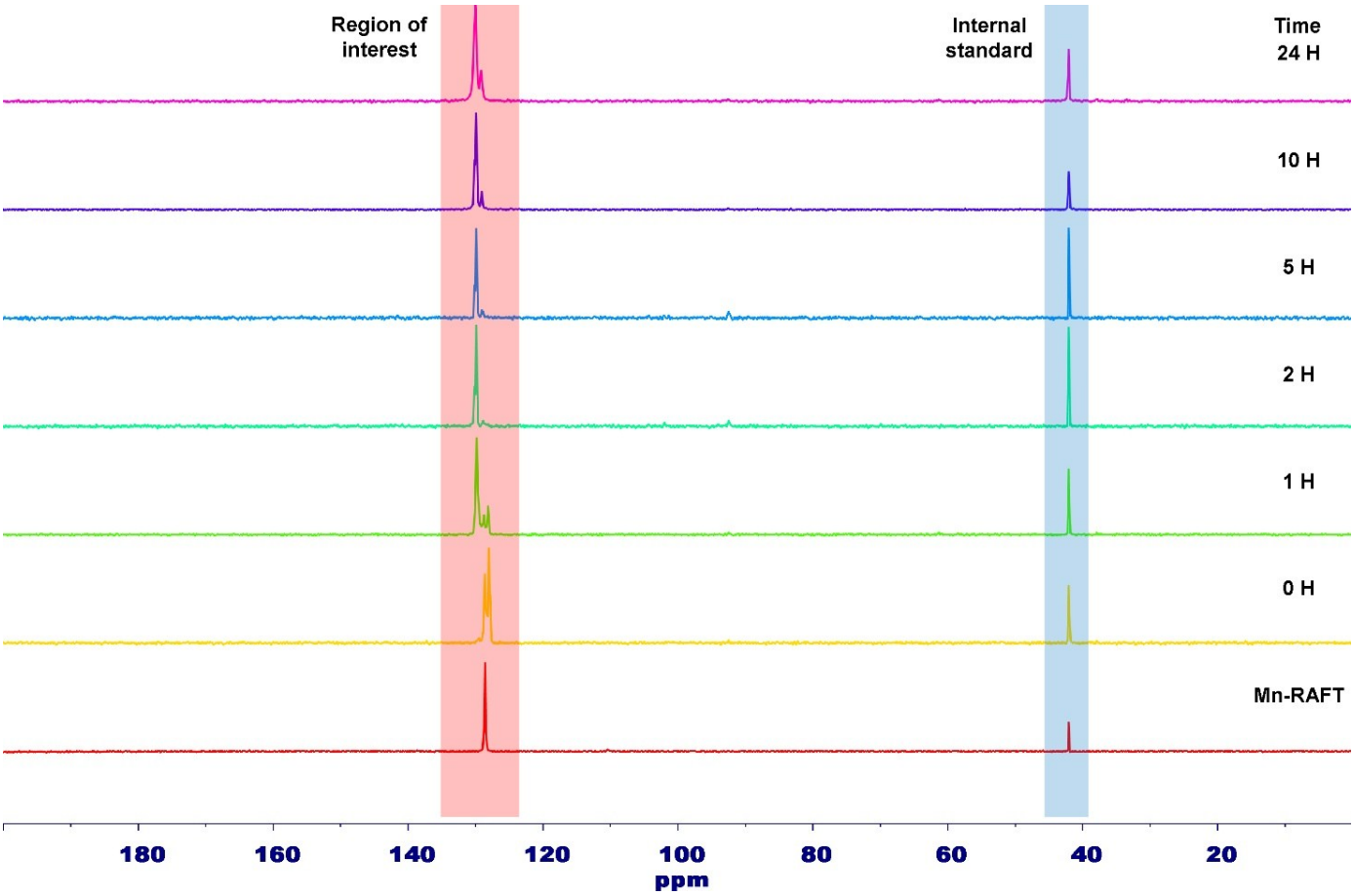

Figure S17. $^{31}P\{^{1}H\}$ NMR spectra obtained during the Mn-RAFT mediated block-copolymerization of St and *n*-BA (121.5 MHz, C_6D_6, 25°C). Each spectrum is fitted to highest intensity.

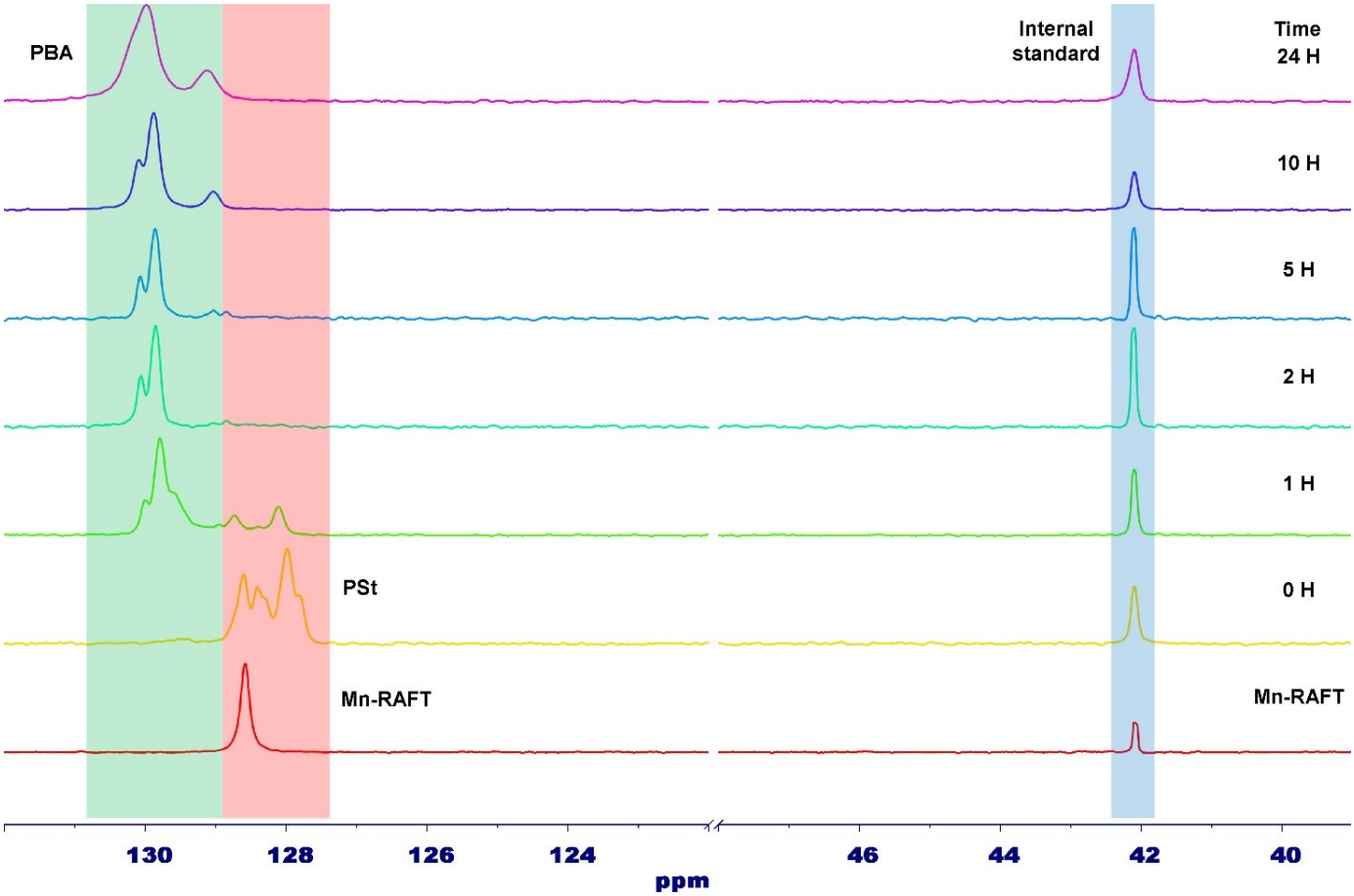

Figure S18. Selected sections of $^{31}P\{^{1}H\}$ NMR spectra obtained during the Mn-RAFT mediated block-copolymerization of St and *n*-BA (121.5 MHz, C_6D_6, 25°C). Each spectrum is fitted to highest intensity.

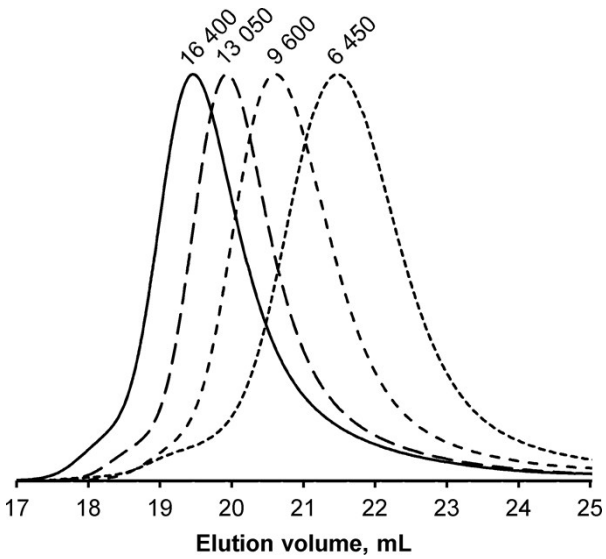

Figure S19. Overlay of SEC chromatograms for the Mn-RAFT polymerization of *n*-BA.

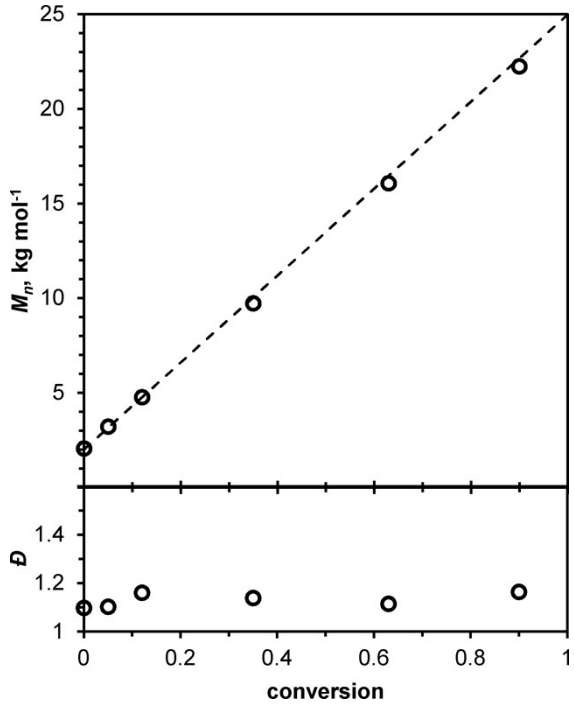

Figure S20. Evolution of M_n and *Đ* during the Mn-RAFT mediated block-copolymerization of St and n-BA.

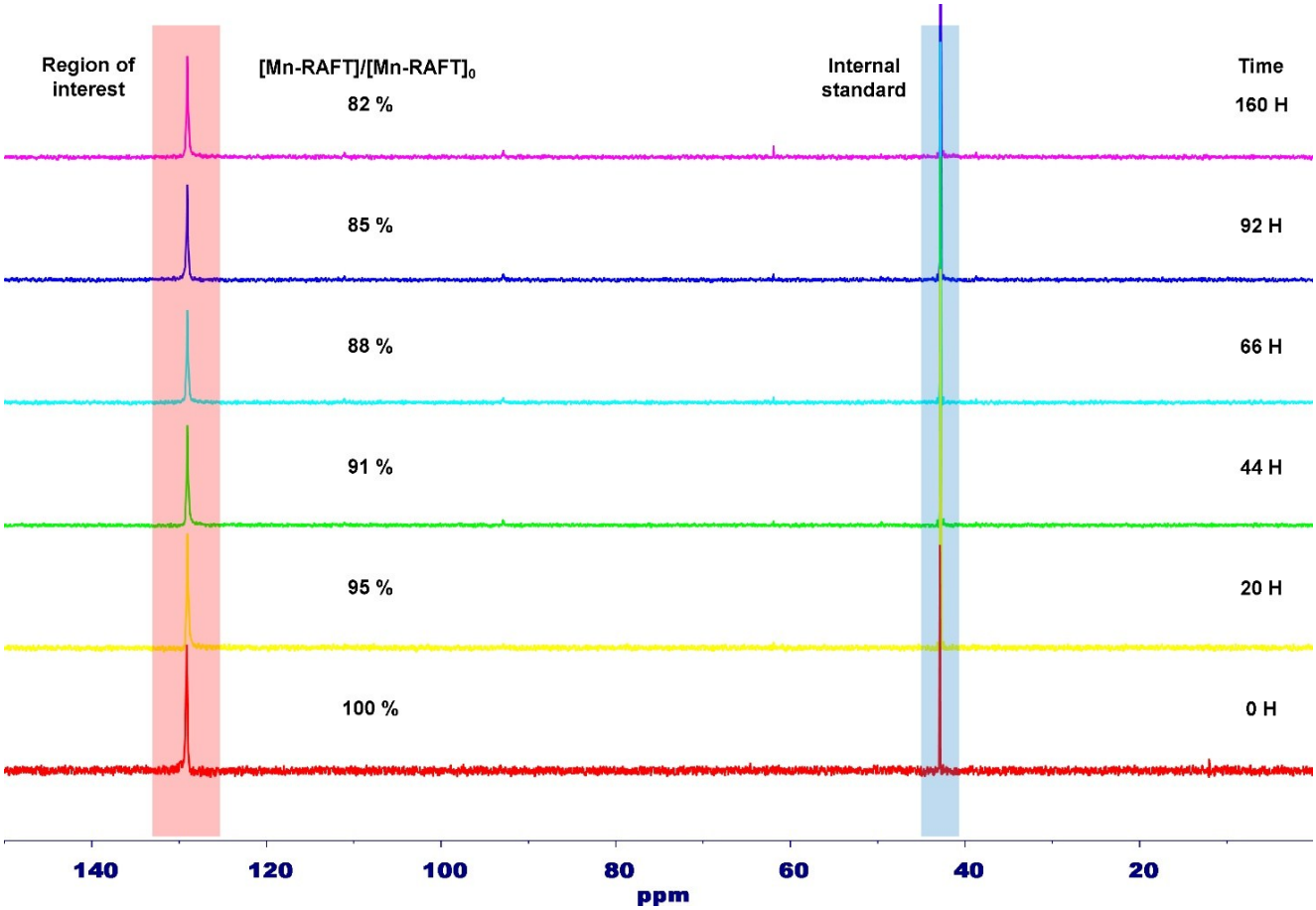

Figure S21. $^{31}P\{^{1}H\}$ NMR monitoring of Mn-RAFT thermolysis in C_6D_6 at 60°C (121.5 MHz, C_6D_6, 25°C).

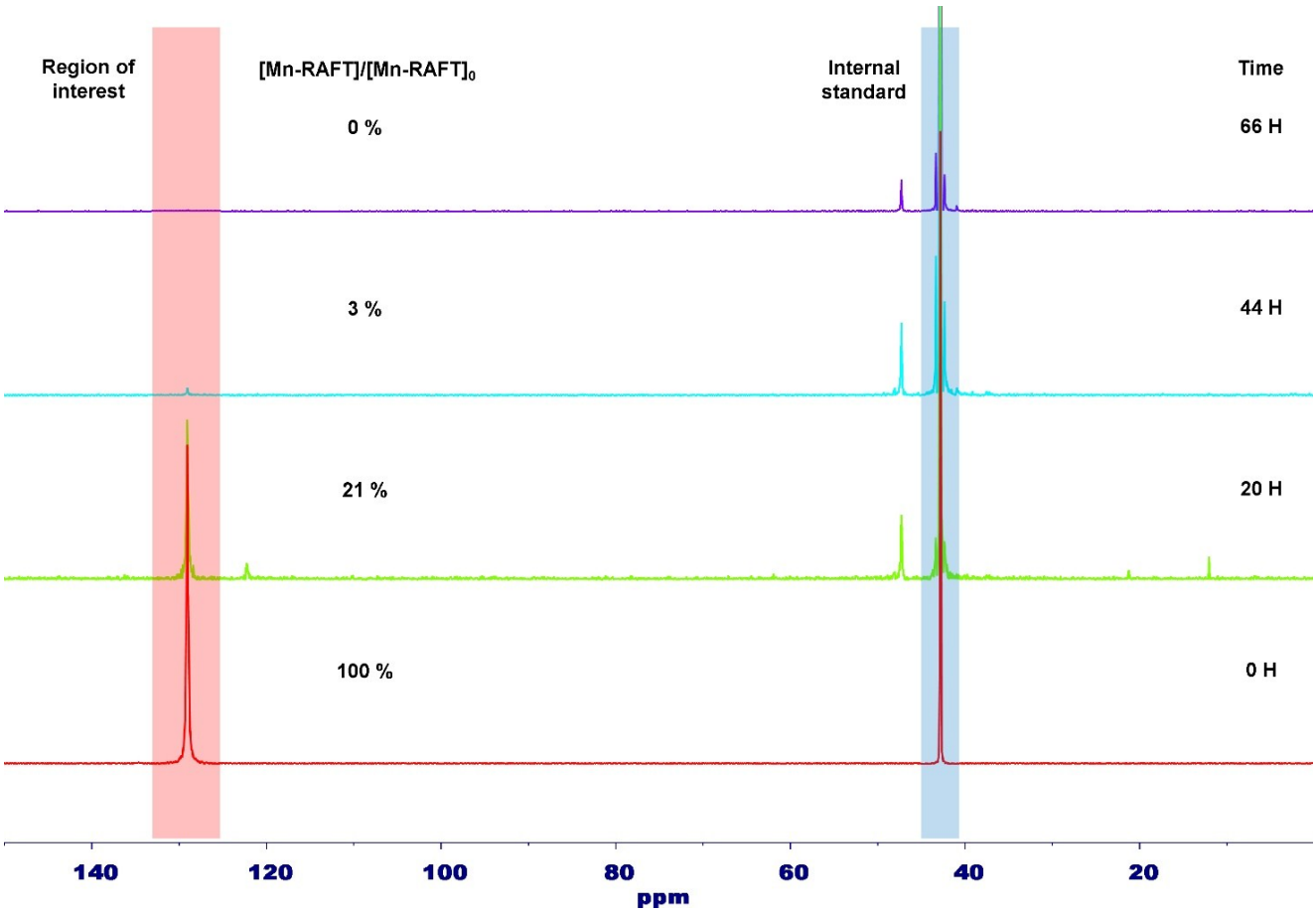

Figure S22. $^{31}P\{^{1}H\}$ NMR monitoring of Mn-RAFT under visible light in C_6D_6 at 60°C (121.5 MHz, C_6D_6, 25°C).

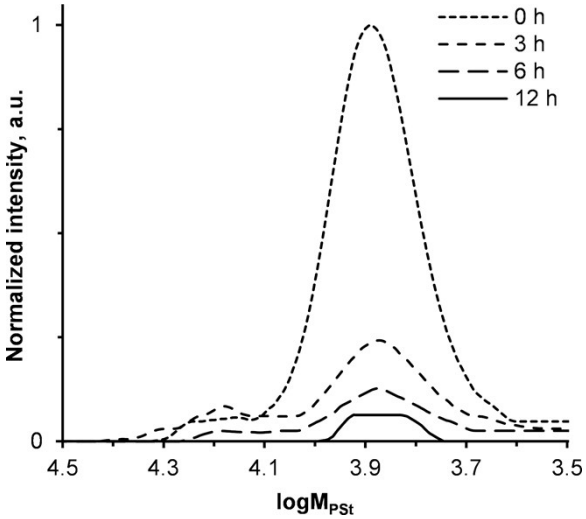

Figure S23. Overlay of SEC chromatograms for the photolysis of PSt sample with UV detection at 290 nm. Signal intensities are normalized by integral intensity of the corresponding SEC-RI trace.

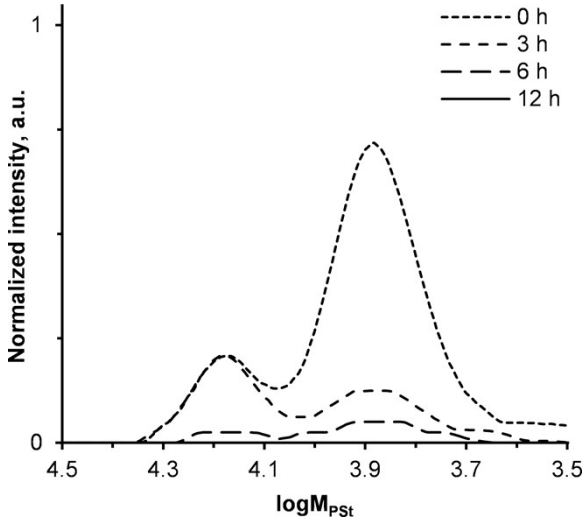

Figure S24. Overlay of SEC chromatograms for the photolysis of PSt sample with UV detection at 310 nm. Signal intensities are normalized by integral intensity of the corresponding SEC-RI trace.

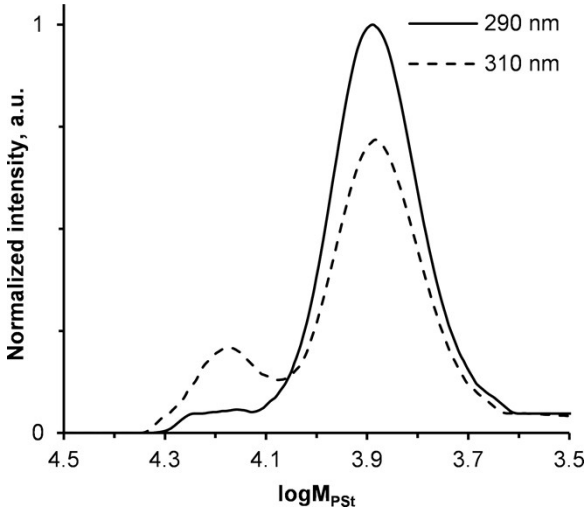

Figure S25. SEC chromatograms of the PSt sample with UV detection at 290 and 310 nm. Signal intensities are normalized by integral intensity of the corresponding SEC-RI trace.

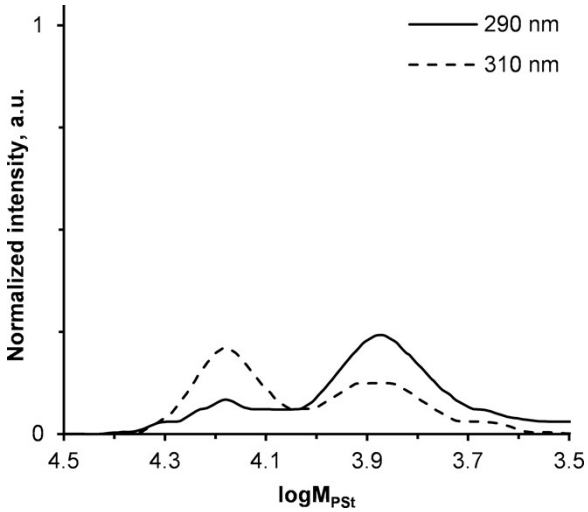

Figure S26. SEC chromatograms of the PSt sample after 3 hours of photolysis with UV detection at 290 and 310 nm. Signal intensities are normalized by integral intensity of the corresponding SEC-RI trace.

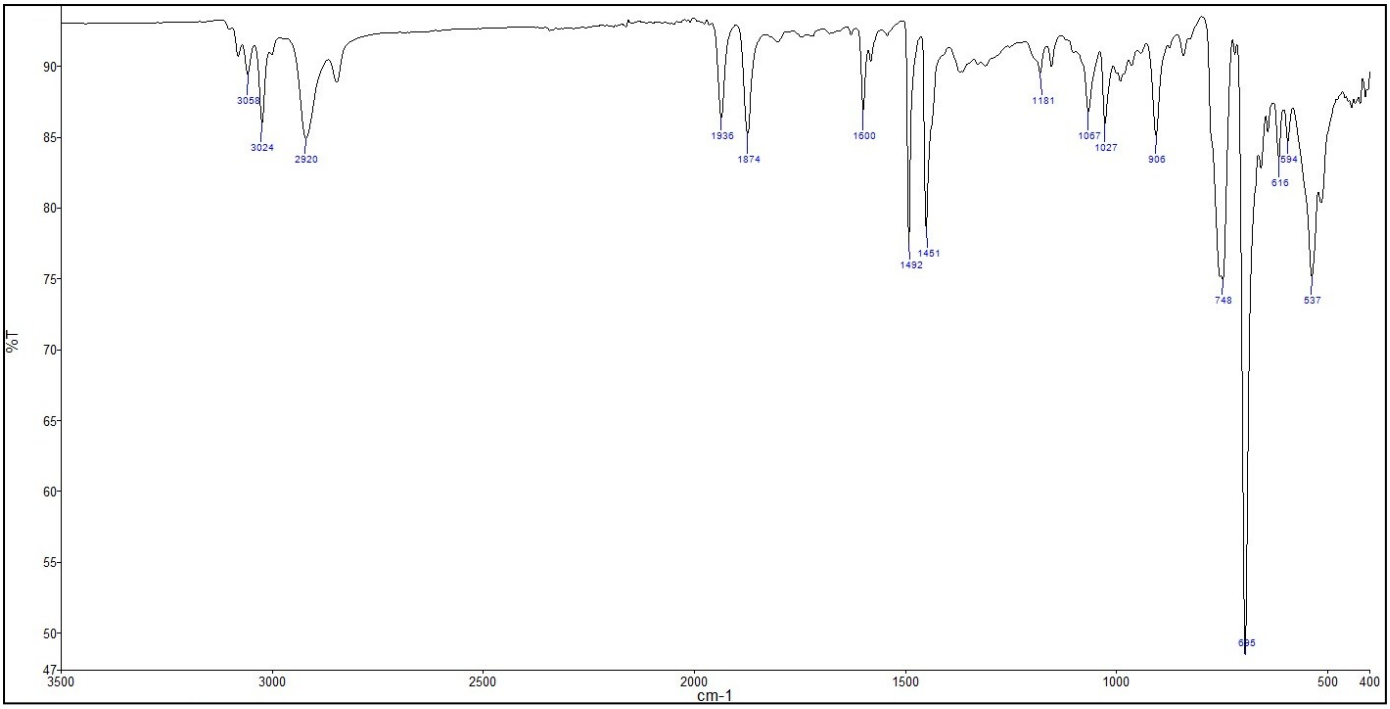

Figure S27. IR spectrum (solid) of Mn-PSt 8.7 kDa (+17.4 kDa)

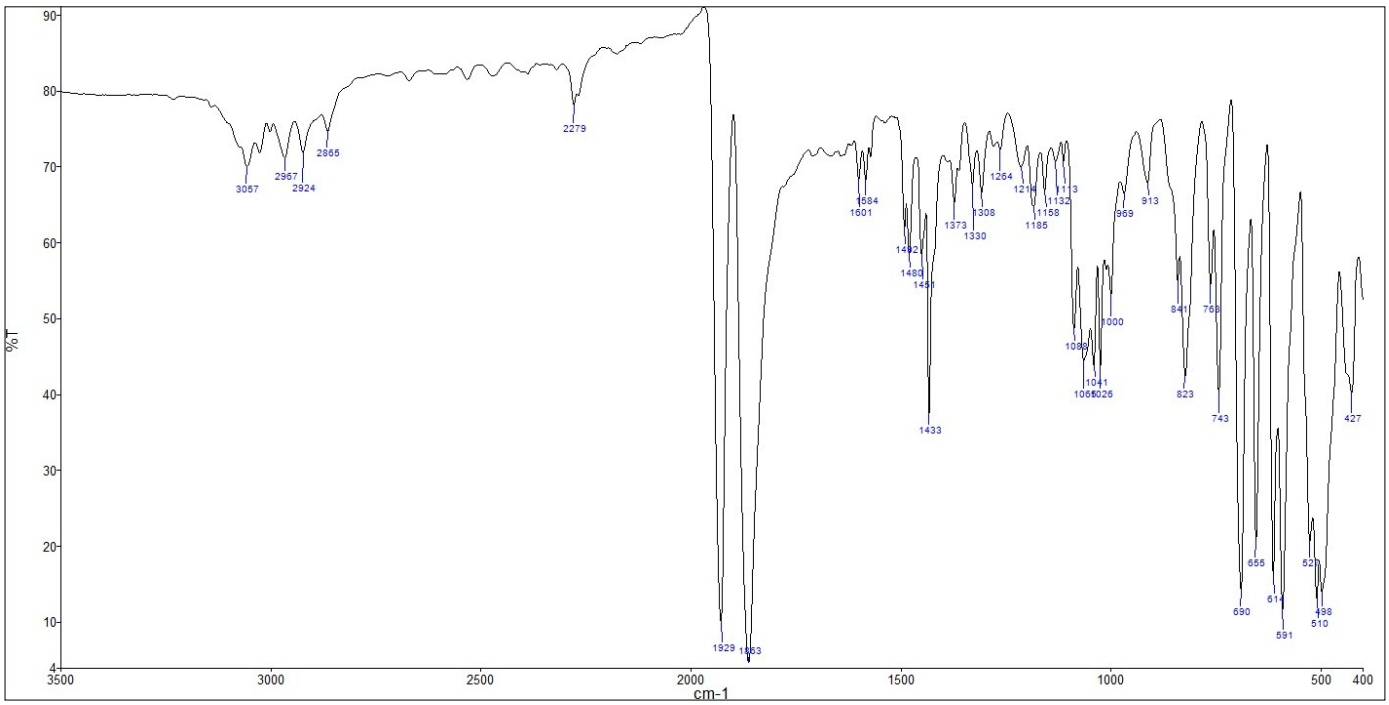

Figure S28. IR spectrum (solid) of Mn-RAFT.

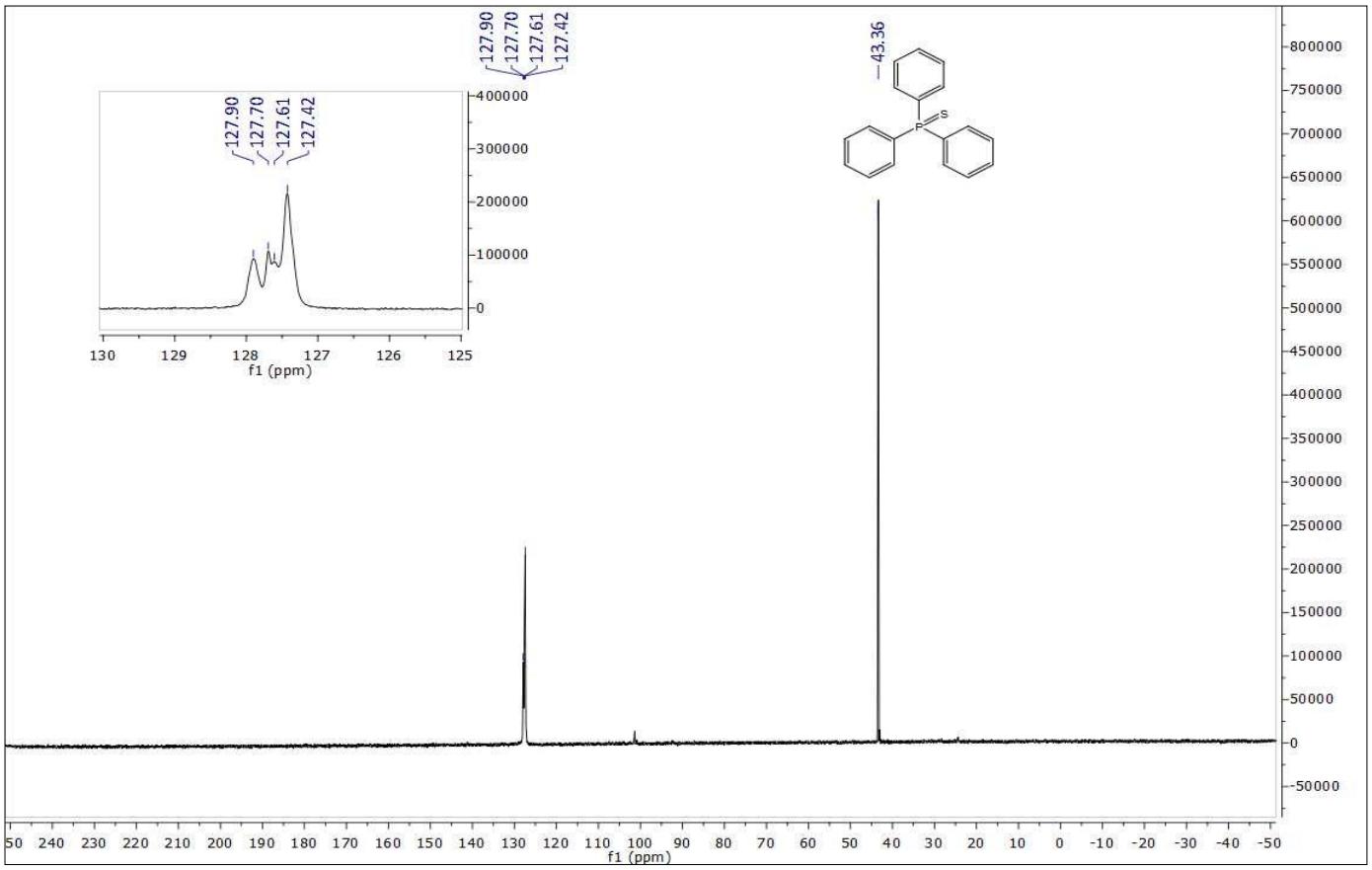

Figure S29. $^{31}P\{^{1}H\}$ NMR spectrum of Mn-PSt 8.7 kDa (+17.4 kDa) (121.5 MHz, $CDCl_3$, 25°C).

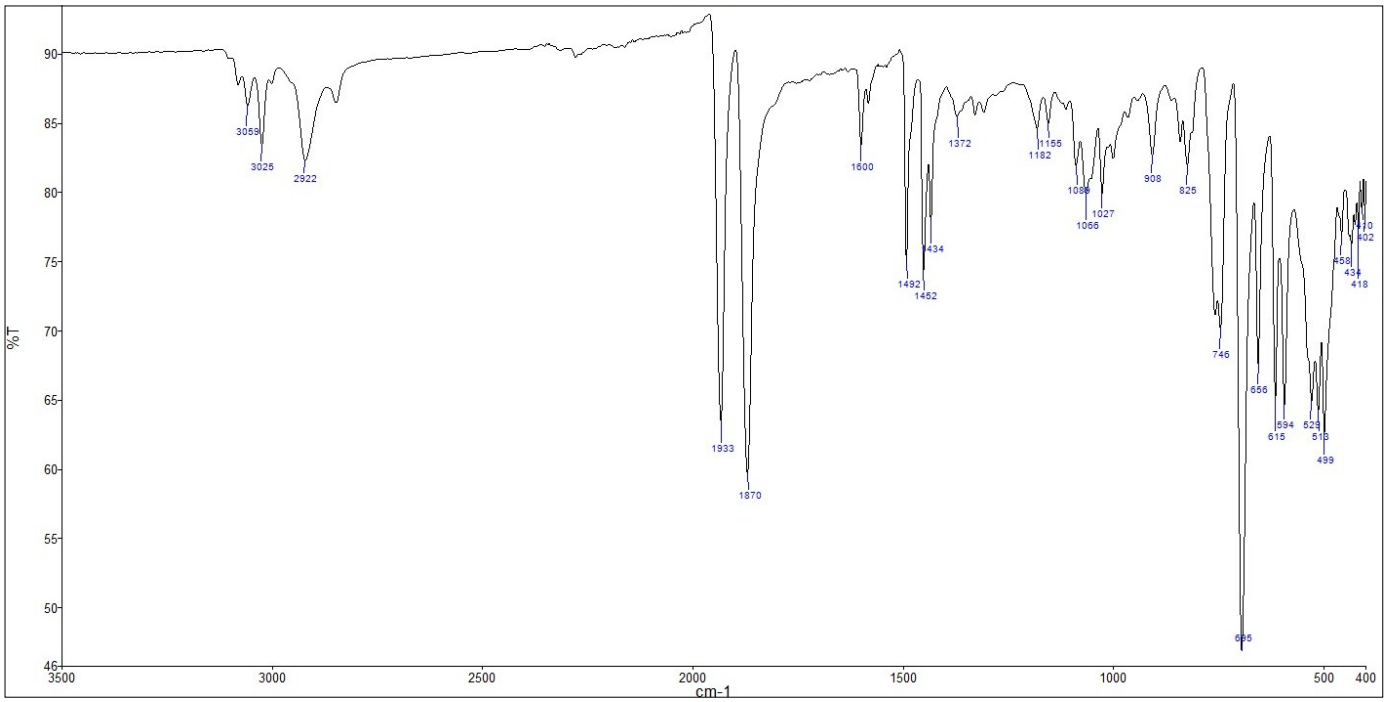

Figure S30. IR spectrum (solid) of Mn-PSt 1.0 kDa.

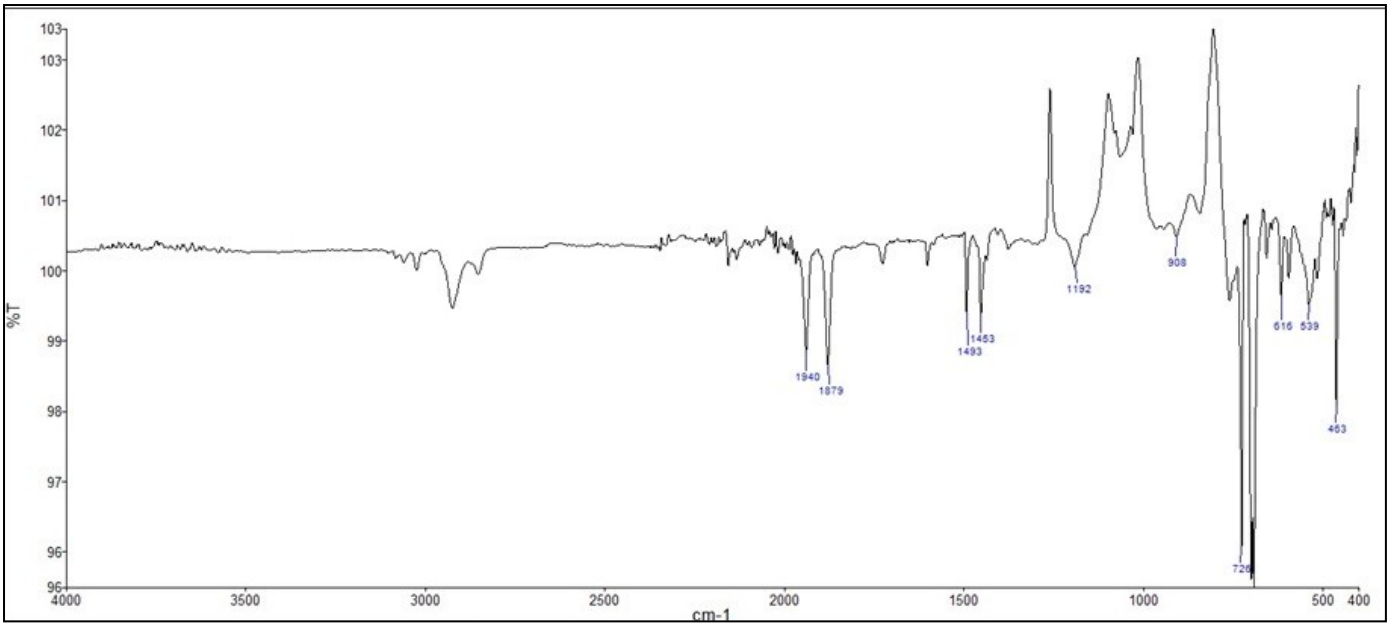

Figure S31. IR spectrum (solution) of Mn-PSt 2.1 kDa.

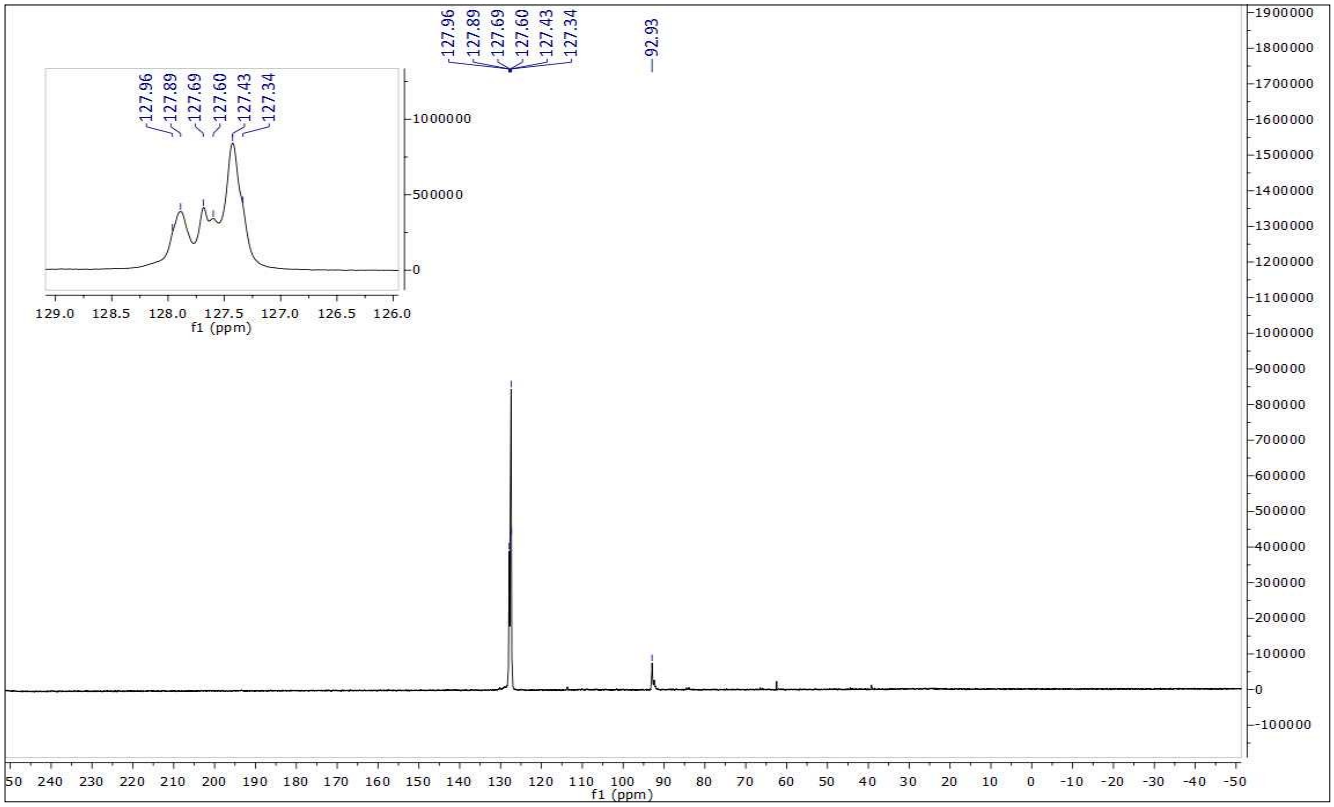

Figure S32. $^{31}P\{^{1}H\}$ NMR spectrum of Mn-PSt 1.0 kDa (121.5 MHz, $CDCl_3$, 25°C).

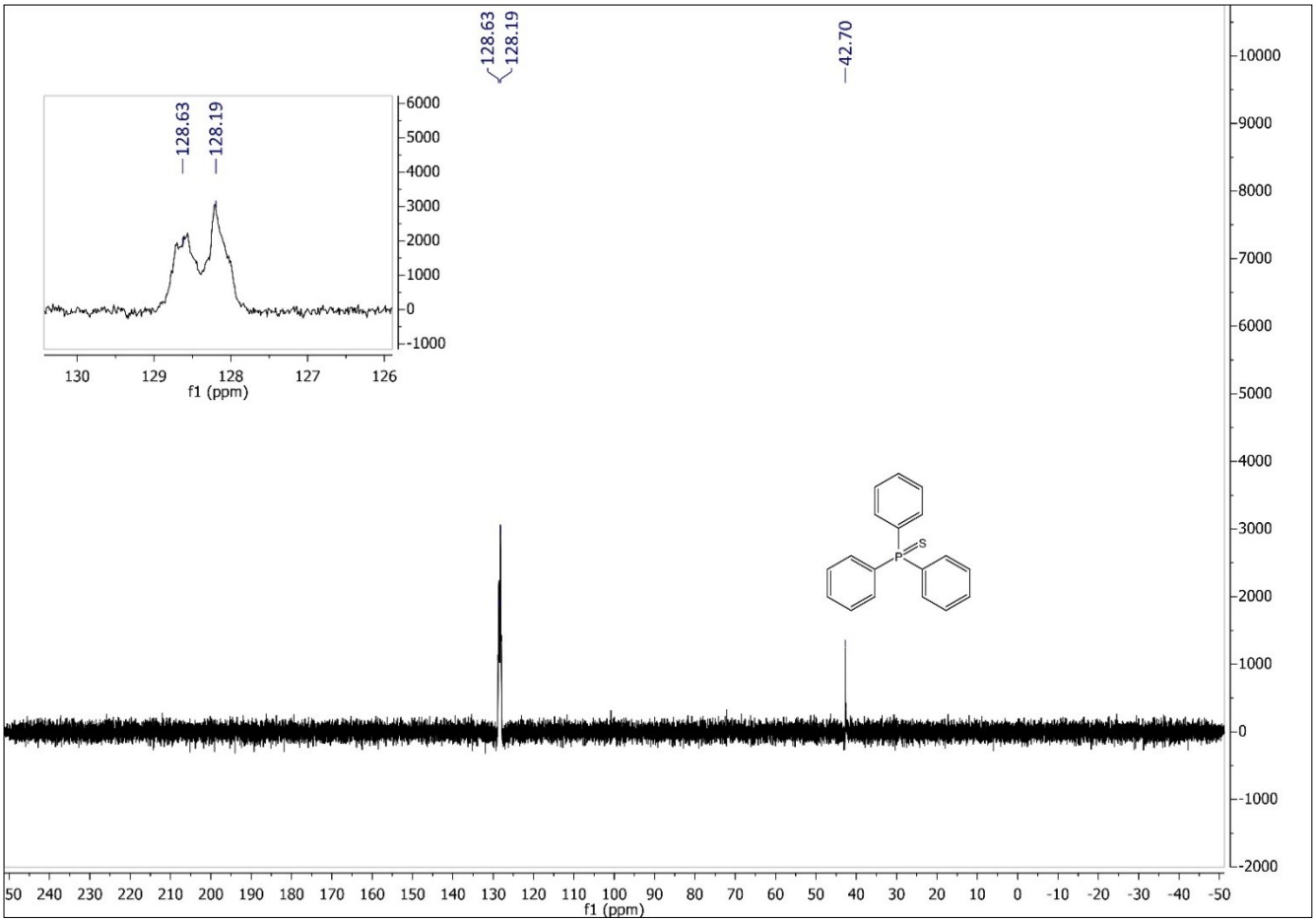

Figure S33. $^{31}P\{^{1}H\}$ NMR spectrum of Mn-PSt 2.1 kDa (121.5 MHz, $CDCl_3$, 25°C).

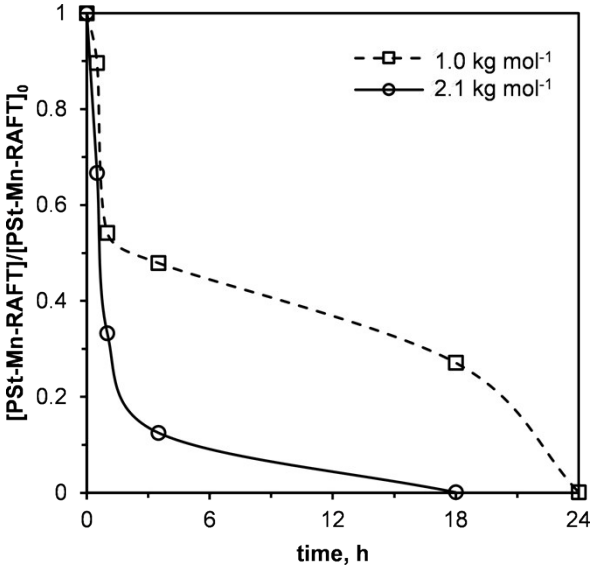

Figure S34. Kinetic plots for photodegradation of PSt samples with M_n of 1.0 kg mol^{-1} and with M_n of 2.1 kg mol^{-1}.

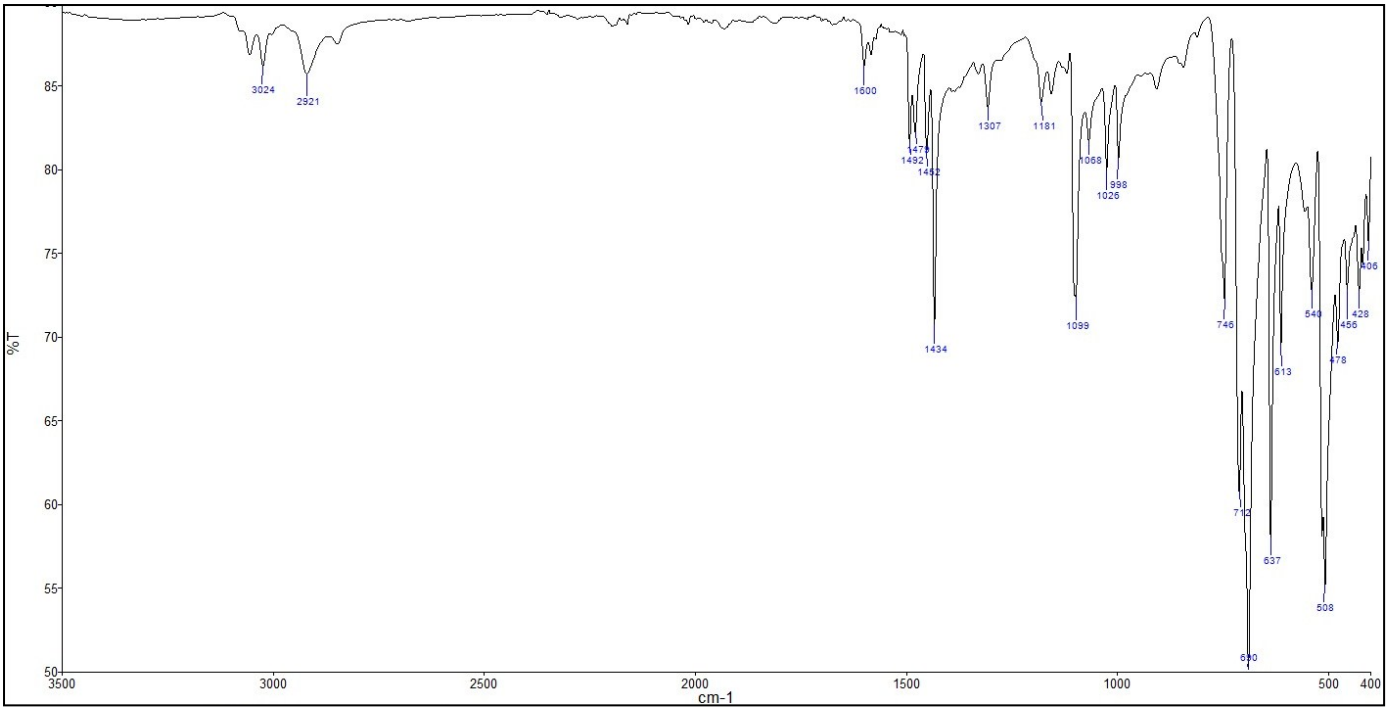

Figure S35. IR spectrum (solid) of Mn-PSt 1.0 kDa after photolysis.

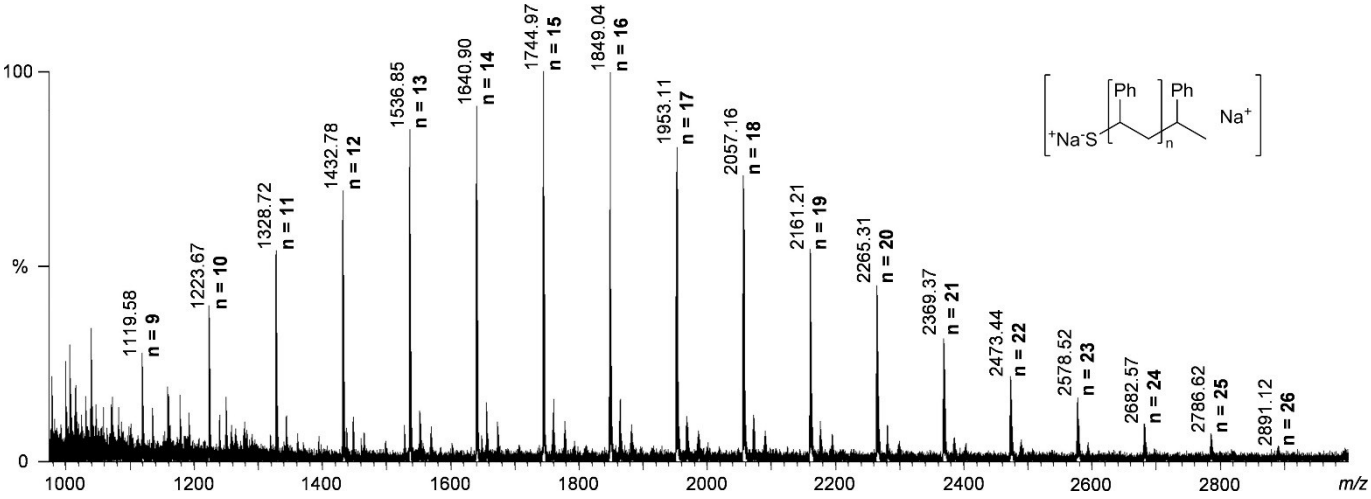

Figure S36. MALDI-TOF spectrum in Ditranol-NaI of the product from photolysis of PSt sample with M_n of 2.1 kg mol^{-1}.

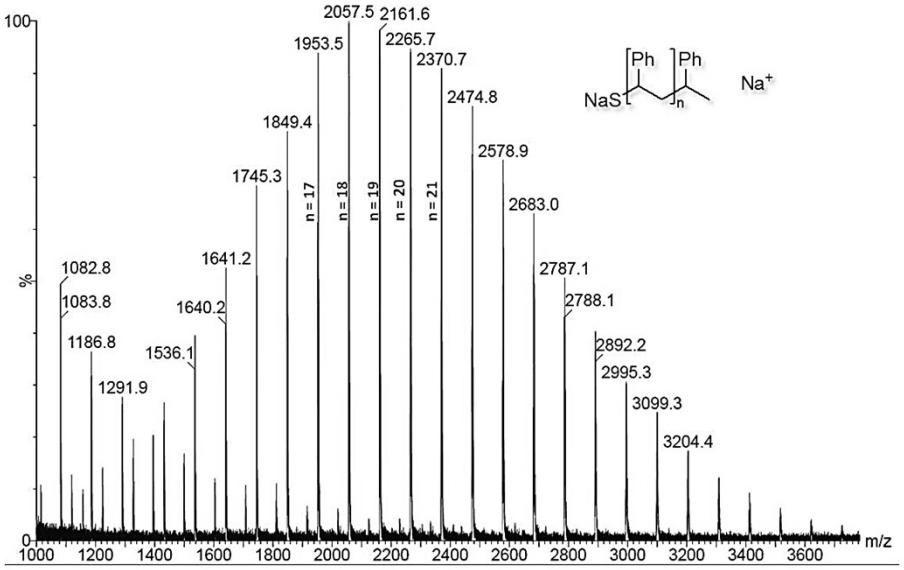

Figure S37. MALDI-TOF spectrum in DCTB-NaI of PSt-Mn-RAFT sample with M_n of 2.1 kg mol^{-1}.

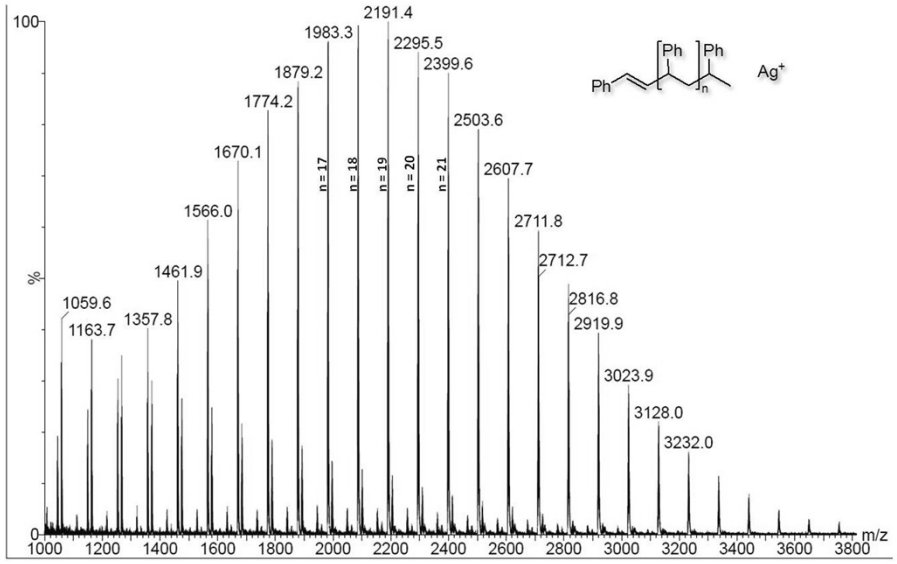

Figure S38. MALDI-TOF spectrum in DCTB-AgOTf of PSt-Mn-RAFT sample with M_n of 2.1 kg mol^{-1}.

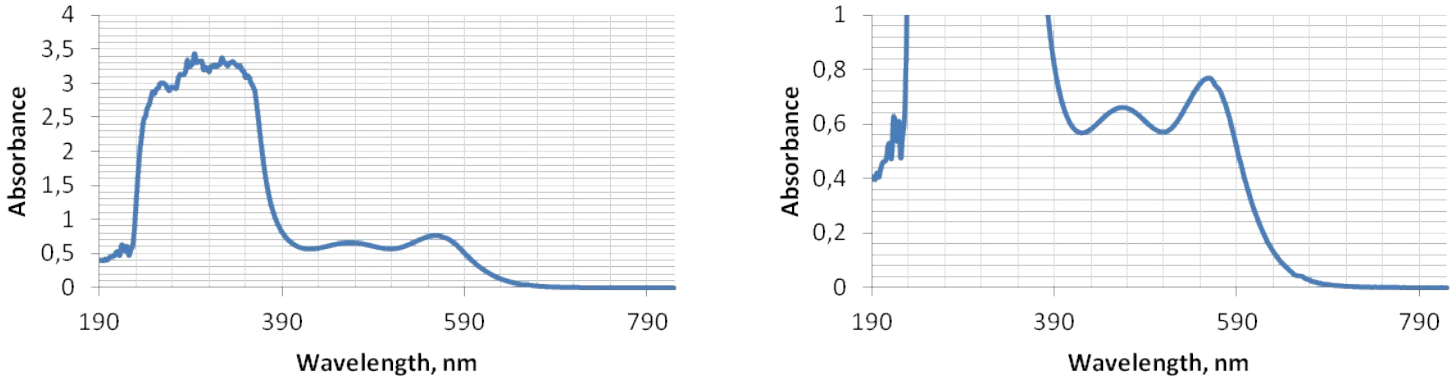

Figure S39. (Left) UV-Visible spectrum of Mn-RAFT in CH_2Cl_2, c = 1.11 mmol.L^{-1}. (Right) Zoom on the two absorption maxima in the visible region. λ nm (ε): 460 (600); 560 (700).